Table 4 Case list for hepatitis B with fatal outcome

Case no.	ISR no.	Reporting year	Age (years)	Gender	Fulminant hepatitis	Time[a] to onset (day)	Reporting country	Medications[b]
1	4390543	2004	72	F	Y	642		**Methotrexate**, prednisolone, bucillamine, alfacalcidol, aspartate calcium, diclofenac sodium, loxoprofen, etidronate disodium
2	4426329	2004	72	F	Y	660		**Methotrexate**, bucillamine
3	4456948	2004	73	M	N	857		**Methotrexate**, prednisolone, alfacalcidol, cimetidine, loxoprofen sodium, benexate hydrochloride, tocopheryl acetate
4	4557482	2005	46	F	Y			**Ciclosporin**, mycophenolate mofetil, lamivudine, methylprednisolone, hydroxychloroquine
5	4694199	2005	69	M	N			Leflunomide, methotrexate
6	4944064	2006		F	N		Japan	Infliximab, methotrexate, isoniazid, prednisolone, loxoprofen sodium, pyridoxal phosphate, risedronate sodium, folic acid, cromoglycate sodium, adrenal cortical extract, polaprezinc
7	4968781	2006		F	N	210	United states	**Etanercept**, prednisone, folic acid
8	4990145	2006	70	F	N	209	United states	**Rofecoxib**, celecoxib, bucindolol hydrochloride, paracetamol
9	5223704	2007		F	N		United kingdom	Infliximab, methotrexate, prednisolone, calcium, dextropropoxyphene, diclofenac sodium, insulin, ranitidine, tramadol hydrochloride
10	5402929	2007		F	N	61	Japan	**Etanercept**, tacrolimus, prednisolone, diclofenac, etodolac, methotrexate, isoniazid, folic acid, aluminium hydroxide, valsartan, alfacalcidol, famotidine
11	5631719	2008	66	F	N	2760	Democratic People's Republic of Korea	**Methotrexate**, prednisolone
12	5636864	2008	66	F	N	2760	Democratic People's Republic of Korea	**Prednisolone**, methotrexate
13	5638752	2008	66	F	N	102	Japan	**Tacrolimus**, prednisolone, methotrexate, etanercept, etodolac, diclofenac, isoniazid, infliximab, folic acid, aluminium hydroxide, valsartan, amlodipine, alfacalcidol, famotidine
14	5652557	2008		F	N	2520	Korea, Republic of	**Methotrexate**, prednisolone
15	5727154	2008	66	F	N		Korea, Republic of	**Methotrexate**, prednisolone
16	5735544	2008	66	F	N	2809		**Methotrexate**, prednisolone, lamivudine
17	5764232	2008		F	N	1402	Taiwan, Province of China	**Etanercept**, methotrexate, sulfasalazine, hydroxychloroquine, felodipine
18	5810978	2008	66	F	N	2789	United states	**Methotrexate**
19	6692841	2010	71	F	N		Japan	**Adalimumab**, methotrexate, prednisolone
20	6782657	2010	50	M	N	990	Japan	**Ciclosporin**, prednisolone, methotrexate
21	6858473	2010	75	F	N	166	United states	**Alendronate sodium**, dextropropoxyphene napsylate, methotrexate, simvastatin, lisinopril, folic acid, prednisone, amoxicillin, levofloxacin, insulin glargine, acyclovir, nystatin, hydrochlorothiazide, rabeprazole sodium, risedronate sodium

Table 4 continued

Case no.	ISR no.	Reporting year	Age (years)	Gender	Fulminant hepatitis	Time[a] to onset (day)	Reporting country	Medications[b]
22	6919632	2010	54	M	Y		Japan	**Tacrolimus**, adalimumab, methotrexate, prednisolone, sulfasalazine, isoniazid, aspartate calcium, alfacalcidol, teprenone, alendronate sodium, raloxifene, mecobalamin, clarithromycin, bromhexine hydrochloride, ambroxol hydrochloride, cromoglycate sodium, fluticasone propionate, tiotropium bromide
23	6928798	2010	71	F	Y	307	Japan	**Adalimumab**, prednisolone, methotrexate, brotizolam, teprenone, famotidine, folic acid, alfacalcidol
24	7009255	2010	69	M	N		United states	Leflunomide, methotrexate, diflunisal
25	7019242	2010	56	M	N	157	Taiwan, Province of China	**Etanercept**
26	7074246	2010	81	F	N		Japan	Infliximab, methotrexate, folic acid, cyanocobalamin, prednisolone, sulfamethoxazole, rabeprazole sodium, acetylsalicylic acid, warfarin, torsemide, potassium canrenoate, estazolam
27	7098562	2010	70	F	N		Japan	Infliximab, methotrexate, prednisolone, adalimumab

ISR no. is a unique number for identifying an AERS report

[a] Period between beginning of primarily suspected drug and onset of reported hepatitis B

[b] Reported primarily suspected drugs are indicated in bold

TNF-α-blocking agents in our analysis, several possible factors could be postulated to affect the differences. First, the differences in dose, dosing schedule, route of administration, or half-life of each agent, as well as potential immunogenicity and synergy effects of frequently administered concomitant medications such as MTX, could to some extend contribute to the findings [24–26]. Differences in their direct toxic effect on hepatocytes without viral reactivation could differently affect the reporting of clinically observed HBV reactivation among TNF-α-blocking agents. When compared with nonbiologic DMARDs, IFX was more frequently associated with elevated liver enzymes more than twice upper limit of normal (OR 2.40, 95 % CI 1.53–3.67), whereas ADA was reported to be less frequently associated (OR 1.72, 95 % CI 0.99–3.01) [27].

Another possible reason for the relative low reporting is that physicians would have avoided using these agents for HBV-infected patients, at least after the risk communications by the ACR, the health authority, and the market authorization holders. However, the latter reason appears to affect to the result only modestly because of our following observation. We reviewed ADA-treated cases from the United States and found that OR of HBV to other AE reports before and after the risk communication by the ACR in 2008 were 1/6,973 and 1/7,569, respectively. OR for prerisk compared with postrisk communication was 1.1 (95 % CI 0.0–39.6), and 1-tailed *P* value for the Fisher exact test was 0.729. Similarly, we compared these ORs for all reporting countries, including the United States, before and after the risk communication by the ACR. After the risk communication, HBV reporting did not decrease. Thus, the risk communication did not appear to affect the reporting of HBV. The prescribers' information for ADA does not contraindicate its use to HBV-infected patients in the United Sates. Moreover, prevalence of HBcAb, which reflects previous or chronic HBV infection, was estimated to range from 5.0 % to 9.1 % in people 50 years or older the United States [28]. Thus, nonnegligible numbers of HBV-infected patients are presumed to be treated with ADA in the United Sates. Nevertheless, the reporting of HBV associated with ADA was very limited, regardless of risk communication.

In this analyses, biologics except for RTX indicated rather low ROR value. As the results are inconclusive, we do not insist that biologics with low ROR are safe for HBV carriers due to various limitations of the spontaneous reporting system. Further investigations are needed to clarify safer use of antirheumatic agents in patients with or previously infected by HBV. Some small observational studies reported safety of anti-TNF treatment in RA

Table 5 Comparison of factors that may affect hepatitis B among tumor necrosis factor-alpha (TNF-α)-blocking biologics

Variables	Adalimumab		Etanercept		Infliximab	
	Hepatitis B ($n = 6$)	Other AE ($n = 29,326$)	Hepatitis B ($n = 38$)	Other AE ($n = 43,788$)	Hepatitis B ($n = 15$)	Other AE ($n = 13,119$)
Mean age (years)	70.7	60.8	58.6	58.4	57.1	61.0
(95 % confidence interval)	(69.2–72.1)	(59.5–62.1)	(53.7–63.6)	(57.9–58.8)	(44.0–70.3)	(60.6–61.3)
Gender						
Male	1	5,521	9	5,318	5	3,392
Male (%)	16.7	18.8	23.7	12.1	33.3	25.9
(95 % confidence interval)	(0.4–64.1)	(18.3–19.3)	(11.4–40.2)	(11.8–12.5)	(11.8–61.6)	(25.1–26.6)
Concomitant use of						
Corticosteroid						
Case number	4	2,957	9	1,046	6	1,375
Proportion (%)	66.7	10.1	23.7	2.4	40.0	10.5
(95 % confidence interval)	(22.3–95.7)	(9.7–10.4)	(11.4–40.2)	(2.2–2.5)	(16.3–67.7)	(10.0–11.0)
Methotrexate						
Case number	3	4,249	10	1,288	8	2,590
Proportion (%)	50.0	14.5	26.3	2.9	53.3	19.7
(95% confidence interval)	(11.8–88.2)	(14.1–14.9)	(13.4–43.1)	(2.8–3.1)	(26.6–78.7)	(19.1–20.4)
Rituximab						
Case number	0	92	0	74	0	59
Proportion (%)	0.0	0.3	0.0	0.2	0.0	0.4
(95 % confidence interval)	(0.0–45.9)	(0.3–0.4)	(0.0–9.3)	(0.1–0.2)	(0.0–21.8)	(0.3–0.6)
Tacrolimus						
Case number	0	40	4	62	0	26
Proportion (%)	0.0	1.4	10.5	0.1	0.0	0.2
(95 % confidence interval)	(0.0–45.9)	(0.1–0.2)	(2.9–24.8)	(0.1–0.2)	(0.0–21.8)	(0.1–0.3)
Reporting country						
Japan						
Case number	3	359	10	1,070	7	3,587
Proportion (%)	50.0	1.2	26.3	2.4	46.7	27.3
(95 % confidence interval)	(11.8–88.1)	(1.1–1.4)	(13.4–43.1)	(2.3–2.6)	(21.3–73.4)	(26.6–28.1)

AE adverse events

patients [5, 6, 8, 29, 30]. If one wants to plan the clinical trial regarding this issue, use of agents with a low indication value could be justified. In such a case, we recommend first considering the use of nucleoside analogs, according to the guidelines [9] and other available information [1, 30].

There was a relatively small number of reports regarding TAC and RTX. Regardless, these agents are associated high ROR in multivariate analysis. It is wise to protect HBV-infected patients from agents such as TAC and RTX (Table 3). Though a specific combination of two antirheumatic agents was not detected as an indication by multivariate analysis, the use of two or more corticosteroids, MTX, RTX TAC, indicated a high risk [ROR 7.6, (CI 6.0–9.7)]. We also do not recommend using these agents in combination with others. Moreover, fatal HBV cases are mostly observed in patients who received a combination of two or more antirheumatic agents, as shown in Table 4. Under these conditions, ADA could cause fatal HBV reactivation, as could other TNF-α-blocking biologics. If patients must absolutely be treated with a combination of these agents, we recommend reconsidering both risks and benefits and considering the use of nucleoside analogs prior to administering antirheumatic agents, according to virological, serological, and biochemical status of HBV infection.

Conclusion

Characteristics of cases with antirheumatic-agent-associated HBV reported to the FDA AERS database were herein described. Potential risk factors, such as reports from Japan and use of corticosteroids, MTX, RTX, and TAC were indicated. There was no relative high reporting

associated with the use of TNF-α-blocking biologics, such as ADA. However, even so, their use may not be completely safe due to several limitations: As approval of ADA was relatively late, its use has been avoided in HBsAg carriers—at least in Japan. Thus, accumulated knowledge of TNF-α blocking agents possibly accelerated the safer use of agents in this class. Based on this view point, reporting of HBV could most likely be suppressed based on the notoriety. However, the possibility that ADA suppresses HBV reactivation also cannot be denied at this point. Prescribing physicians should not alter their awareness and caution in the use of these agents in RA patients with concurrent or resolved HBV infection based on this single analysis. If ADA really does have a lesser capacity for HBV reactivation, therapeutic options in RA patients with HBV would be expanded. Thus, this attractive possibility appears worth investigation. Until the possibility is clarified in well-designed clinical studies, physicians should use caution when using this agent in patients with HBV. Further investigations are needed to determine the safer use of antirheumatic agents in consideration of HBV infection or reactivation.

Limitations

There are known limitations of spontaneous reporting systems. They comprise underreporting, the Weber-effect, reporting bias, indication bias, and notoriety bias. For example, in our analysis, low ROR associated with ADA is most likely due to the avoidance of its use in HBV carriers. However, the database does not contain enough information to prompt a more detailed discussion regarding screening for HBV virus prior to treatment or antibody/antigen status, such as HBsAg, HBcAb, or DNA replication. For example, of 92 HBV cases, only five and one case was reported, respectively, with HBsAg and HBeAg positivity. Otherwise there is no information that suggests the status of antibody/antigen for HBV.

Conflict of interest The authors report the following funding sources that could have possible relevance to the work described here: Yasuo Oshima, MD, PhD, FACP; a stipend from sanofi-aventis K.K. Hiroshi Tsukamoto, MD, PhD No COI. Arinobu Tojo, MD, PhD; research fund from Novartis Pharma K.K., Bristol-Myers Squibb Company, Chugai Pharmaceutical Co., Ltd., Otsuka Pharmaceutical Co., Ltd., and Dainippon Sumitomo Pharma Co., Ltd. and compensation for an expert testimony from Celgene K.K.

References

1. Calabrese LH, Zein NN, Vassilopoulos D. Hepatitis B virus (HBV) reactivation with immunosuppressive therapy in rheumatic diseases: assessment and preventive strategies. Ann Rheum Dis. 2006;65(8):983–9.
2. Zingarelli S, Airo P, Frassi M, Bazzani C, Scarsi M, Puoti M. Prophylaxis and therapy of HBV infection in 20 patients treated with disease modifying antirheumatic drugs or with biological agents for rheumatic diseases. Reumatismo. 2008;60(1):22–7.
3. Saag KG, Teng GG, Patkar NM, et al. American College of Rheumatology 2008 recommendations for the use of nonbiologic and biologic disease-modifying antirheumatic drugs in rheumatoid arthritis. Arthritis Rheum. 2008;59(6):762–84.
4. Fauci AS, Kasper DL, Longo DL, et al. Harrison's principles of internal medicine. 17th Edition. New York: McGraw-Hill; 2008.
5. Tamori A, Koike T, Goto H, et al. Prospective study of reactivation of hepatitis B virus in patients with rheumatoid arthritis who received immunosuppressive therapy: evaluation of both HBsAg-positive and HBsAg-negative cohorts. J Gastroenterol. 2011;46(4):556–64.
6. Mori S. Past hepatitis B virus infection in rheumatoid arthritis patients receiving biological and/or nonbiological disease-modifying antirheumatic drugs. Mod Rheumatol. 2011.
7. Caporali R, Bobbio-Pallavicini F, Atzeni F, et al. Safety of tumor necrosis factor alpha blockers in hepatitis B virus occult carriers (hepatitis B surface antigen negative/anti-hepatitis B core antigen positive) with rheumatic diseases. Arthritis Care Res (Hoboken). 2010;62(6):749–54.
8. Vassilopoulos D, Apostolopoulou A, Hadziyannis E, et al. Long-term safety of anti-TNF treatment in patients with rheumatic diseases and chronic or resolved hepatitis B virus infection. Ann Rheum Dis. 2010;69(7):1352–5.
9. Tsubouchi H, Kumada H, Kiyosawa K, et al. Prevention of immunosuppressive therapy or chemotherapy-induced reactivation of hepatitis B virus infection Joint report of the Intractable Liver Diseases Study Group of Japan and the Japanese Study Group of the standard antiviral therapy for viral hepatitis. Kanzo. 2009;50(1):38–42.
10. Oshima Y, Tojo A. Pulmonary alveolar hemorrhage possibly associated with lenalidomide use. Int J Hematol. 2011;94(3):296–7.
11. Oshima Y, Tojo A. Attractive tools for systematic case accumulation. Int J Hematol. 2011;94(4):413–4.
12. Murashige N, Tanimoto T, Oshima Y. Interstitial lung disease and gefitinib. N Engl J Med. 2010;363(16):1578–9. author reply 1579–80.
13. Oshima Y. Characteristics of drug-associated rhabdomyolysis: analysis of 8,610 cases reported to the US Food and Drug Administration. Intern Med. 2011;50(8):845–53.
14. Pariente A, Gregoire F, Fourrier-Reglat A, Haramburu F, Moore N. Impact of safety alerts on measures of disproportionality in spontaneous reporting databases: the notoriety bias. Drug Saf. 2007;30(10):891–8.
15. Umemura T, Kiyosawa K. Fatal HBV reactivation in a subject with anti-HBs and anti-HBc. Intern Med. 2006;45(12):747–8.
16. Lok AS, Liang RH, Chiu EK, Wong KL, Chan TK, Todd D. Reactivation of hepatitis B virus replication in patients receiving cytotoxic therapy. Report of a prospective study. Gastroenterology. 1991;100(1):182–8.
17. Hass M, Hannoun C, Kalinina T, Sommer G, Manegold C, Gunther S. Functional analysis of hepatitis B virus reactivating in hepatitis B surface antigen-negative individuals. Hepatology. 2005;42(1):93–103.
18. Rothman KJ, Lanes S, Sacks ST. The reporting odds ratio and its advantages over the proportional reporting ratio. Pharmacoepidemiol Drug Saf. 2004;13(8):519–23.
19. Yeo W, Johnson PJ. Diagnosis, prevention and management of hepatitis B virus reactivation during anticancer therapy. Hepatology. 2006;43(2):209–20.

20. Cheng AL, Hsiung CA, Su IJ, et al. Steroid-free chemotherapy decreases risk of hepatitis B virus (HBV) reactivation in HBV-carriers with lymphoma. Hepatology. 2003;37(6):1320–8.
21. Ishikawa T, Kono D, Chung J, et al. Polyclonality and multi-specificity of the CTL response to a single viral epitope. J Immunol. 1998;161(11):5842–50.
22. Thimme R, Wieland S, Steiger C, et al. CD8(+) T cells mediate viral clearance and disease pathogenesis during acute hepatitis B virus infection. J Virol. 2003;77(1):68–76.
23. Ando K, Moriyama T, Guidotti LG, et al. Mechanisms of class I restricted immunopathology. A transgenic mouse model of fulminant hepatitis. J Exp Med. 1993;178(5):1541–54.
24. Pfizer Japan Inc. Interview form for Eternelcept. In: http://www.info.pmda.go.jp/go/interview/2/671450_3999424G1025_2_1F. 18 ed. Tokyo, Japan; 2012.
25. Mitsubishi Tanabe Pharma Corporation. Interview form for Infliximab. In: http://www.info.pmda.go.jp/go/interview/1/400315_2399402F1026_1_200_1F. 20 ed. Osaka, Japan; 2012.
26. Abbott Japan Co. Ltd. Interview form for Adalimumab. In: http://www.info.pmda.go.jp/go/interview/1/100159_3999426G1024_1_005_1F. 5 ed. Tokyo, Japan; 2010.
27. Strand V, Kimberly R, Isaacs JD. Biologic therapies in rheumatology: lessons learned, future directions. Nat Rev Drug Discov. 2007;6(1):75–92.
28. Ioannou GN. Hepatitis B virus in the United States: infection, exposure, and immunity rates in a nationally representative survey. Ann Intern Med. 2011;154(5):319–28.
29. Li S, Kaur PP, Chan V, Berney S. Use of tumor necrosis factor-alpha (TNF-alpha) antagonists infliximab, etanercept, and adalimumab in patients with concurrent rheumatoid arthritis and hepatitis B or hepatitis C: a retrospective record review of 11 patients. Clin Rheumatol. 2009;28(7):787–91.
30. Benucci M, Manfredi M, Mecocci L. Effect of etanercept plus lamivudine in a patient with rheumatoid arthritis and viral hepatitis B. J Clin Rheumatol. 2008;14(4):245–6.

ErbB receptor tyrosine kinase/NF-κB signaling controls mammosphere formation in human breast cancer

Kunihiko Hinohara[a], Seiichiro Kobayashi[b], Hajime Kanauchi[c], Seiichiro Shimizu[d], Kotoe Nishioka[e], Ei-ichi Tsuji[e], Kei-ichiro Tada[e], Kazuo Umezawa[f], Masaki Mori[g], Toshihisa Ogawa[e], Jun-ichiro Inoue[h], Arinobu Tojo[b], and Noriko Gotoh[a,1]

[a]Division of Systems Biomedical Technology, Institute of Medical Science, University of Tokyo, Minato-ku, Tokyo 108-8639, Japan; [b]Division of Molecular Therapy, Advanced Clinical Research Center, Institute of Medical Science, University of Tokyo, Minato-ku, Tokyo 108-8639, Japan; [c]Department of Breast and Endocrine Surgery, Showa General Hospital, Kodaira-shi, Tokyo 187-8510, Japan; [d]Department of Pathological Diagnosis, Showa General Hospital, Kodaira-shi, Tokyo 187-8510, Japan; [e]Department of Breast and Endocrine Surgery, Graduate School of Medicine, University of Tokyo, Bunkyo-ku, Tokyo 113-8655, Japan; [f]Department of Applied Chemistry, Faculty of Science and Technology, Keio University, Yokohama-shi, Kanagawa 223-8522, Japan; [g]Department of Gastroenterological Surgery, Osaka University, Suita-shi, Osaka, 565-0871, Japan; [h]Division of Cellular and Molecular Biology, Institute of Medical Science, University of Tokyo, Minato-ku, Tokyo 108-8639, Japan

Edited by Joseph Schlessinger, Yale University School of Medicine, New Haven, CT, and approved March 8, 2012 (received for review August 15, 2011)

Breast cancer is one of the most common cancers in humans. However, our understanding of the cellular and molecular mechanisms underlying tumorigenesis in breast tissues is limited. Here, we identified a molecular mechanism that controls the ability of breast cancer cells to form multicellular spheroids (mammospheres). We found that heregulin (HRG), a ligand for ErbB3, induced mammosphere formation of a breast cancer stem cell (BCSC)–enriched population as well as in breast cancer cell lines. HRG-induced mammosphere formation was reduced by treatment with inhibitors for phosphatidyl inositol 3-kinase (PI3K) or NF-κB and by expression of IκBα-Super Repressor (IκBαSR), a dominant-negative inhibitor for NF-κB. Moreover, the overexpression of IκBαSR in breast cancer cells inhibited tumorigenesis in NOD/SCID mice. Furthermore, we found that the expression of IL8, a regulator of self-renewal in BCSC-enriched populations, was induced by HRG through the activation of the PI3K/NF-κB pathway. These findings illustrate that HRG/ErbB3 signaling appears to maintain mammosphere formation through a PI3K/NF-κB pathway in human breast cancer.

EGF | HER | tumor sphere | cancer stem cells | inflammation

Cancer stem cells (CSCs), which make up only a small proportion of heterogeneous tumor cells, may possess a greater ability to maintain tumorigenesis than other tumor cell types (1, 2). CSCs can self-renew and simultaneously produce differentiated daughter cells; thus they can strongly proliferate until they reach their final differentiated state. With improvements in the isolation of CSCs, there is now a growing body of evidence that, in some cases of hematologic and solid tumors, a cancer stem cell population can be enriched based on phenotype (3–10). In human breast cancers, breast cancer stem cells (BCSCs) are enriched in the $CD44^{high}/CD24^{low}$ cell population, whereas the $CD44^{low}/CD24^{high}$ cells represent a more differentiated phenotype with limited stem cell–like potential (3). Because BCSCs withstand anoikis in culture, they expand under anchorage-independent conditions, giving rise to clonal spheroids (mammospheres), which can be serially passaged in vitro (11, 12). These processes can in part recapitulate the breast tumorigenesis process (13–16). To develop more effective cancer therapies, it would be reasonable to target molecules that have a critical role in the maintenance of mammospheres. However, the molecular mechanism by which mammospheres are maintained is still largely obscure.

NF-κB is a transcription factor complex that is typically a heterodimer of p50, p52, p65 (RelA), RelB, and c-Rel. It is usually inactive and bound to IκB, an inhibitory protein, in the cytoplasm. The primary mechanism of regulation of NF-κB activity is through activation of the IKK complex, including heterodimers of IKKα and IKKβ, as a result of various signaling pathways. The serine–threonine kinase Akt is one of the activators of IKKβ (17), and the activated IKK complex phosphorylates the IκBα protein, resulting in its ubiquitination, proteasome-mediated degradation, and subsequent release of NF-κB for nuclear translocation. Released NF-κB translocates to the nucleus and binds to the κB sequence, where it promotes the transcription of various genes, including inflammatory chemokines. Recently, we found activation of inflammatory signaling pathways in association with an increase in NF-κB activity in BCSC-enriched populations (18, 19). However, the role of NF-κB and the molecular mechanisms by which NF-κB is activated during mammosphere formation remain unknown.

Heregulin (HRG, also called neuregulin) is a ligand for ErbB3, which is one of the four members of the EGF receptor ErbB family (20). Expression of HRG in the mammary gland induces adenocarcinomas in animal models (21) and favors metastatic spread of breast cancer cells (22). HRG is expressed in 30% of human breast cancer patients (23) and correlates with poor histological grade (24). Recently, it was reported that ErbB2 overexpression increases the stem/progenitor cell population of both normal and malignant mammary cells (25); however the role of HRG and ErbB3 in regulating the properties of BCSC-enriched populations remains largely unknown.

In the present study, we showed that HRG induced mammosphere formation of cancer cells from a BCSC-enriched population. Moreover, our findings suggest that the activity of phosphatidyl inositol 3-kinase (PI3K)/NF-κB is essential for the HRG-induced mammosphere formation.

Results

HRG Induces Mammosphere Formation of a BCSC-Enriched Population. To test the mammosphere-forming ability of a BCSC-enriched population, we initially isolated $CD44^{high}/CD24^{low}/lineage^-$ BCSC-enriched population and $CD44^{low}/CD24^{high}/lineage^-$ nonstem cells from human breast cancer tissue. When these cells were cultured with conventional mammosphere culture media containing EGF, bFGF, and B27 supplement (13, 26), the $CD44^{high}/CD24^{low}/lineage^-$ BCSC-enriched population generated mammospheres, whereas the $CD44^{low}/CD24^{high}/lineage^-$ nonstem cells did not form mammospheres (Fig. 1 *A* and *B*). These observations suggest that cells with the capacity to

Author contributions: K.H. and N.G. designed research; K.H. performed research; S.K., H.K., S.S., K.N., E.-i.T., K.-i.T., K.U., M.M., T.O., J.-i.I., and A.T. contributed new reagents/analytic tools; K.H. analyzed data; and K.H. and N.G. wrote the paper.

The authors declare no conflict of interest.

This article is a PNAS Direct Submission.

Freely available online through the PNAS open access option.

[1]To whom correspondence should be addressed. E-mail: ngotoh@ims.u-tokyo.ac.jp

This article contains supporting information online at www.pnas.org/lookup/suppl/doi:10.1073/pnas.1113271109/-/DCSupplemental.

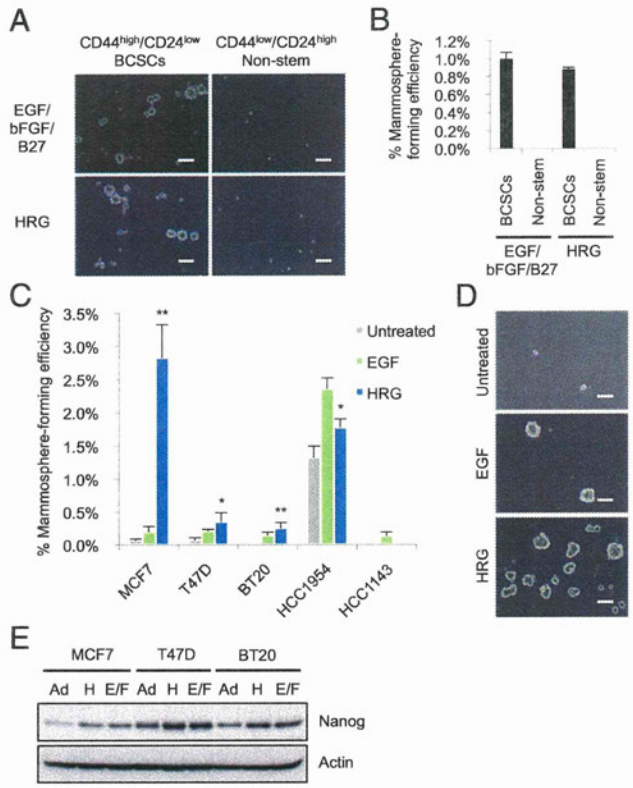

Fig. 1. Effect of HRG on mammosphere formation of a BCSC-enriched population. (*A*) Representative images of primary cultures of mammospheres formed from the sorted $CD44^{high}/CD24^{low}$/lineage$^-$ BCSC-enriched population (*Left*) and the $CD44^{low}/CD24^{high}$/lineage$^-$ nonstem cell population (*Right*) obtained from a specimen of invasive ductal carcinoma (IDC1, Table S1). The cells from IDC1 were incubated with EGF/bFGF/B27 (*Top*) or with 20 ng/mL HRG (*Bottom*). Scale bar = 100 μm. (*B*) The spheres were counted and the percentage of mammosphere-forming cells were determined in each group (data are mean ± SD; $n = 4$). (*C*) Mammosphere assay in MCF7, T47D, BT20, HCC1954, and HCC1143 breast cancer cell lines treated with 20 ng/mL EGF or 20 ng/mL HRG (data are mean ± SD; $n = 4$, $^{**}P < 0.01$, $^{*}P < 0.05$, relative to the values in the respective untreated controls). (*D*) Images showing mammosphere formation in MCF7 cells treated as indicated in (*C*). Scale bar = 100 μm. (*E*) Nanog protein expression levels in the parental cells growing in 2D adherent (Ad) culture, sphere cells cultured with 20 ng/mL HRG (H) and sphere cells cultured with EGF/bFGF/B27 (E/F).

form mammospheres are enriched in $CD44^{high}/CD24^{low}$/lineage$^-$ cells, confirming that mammospheres can be derived from BCSC-enriched populations as described previously (26, 27).

To examine the effects of HRG on the mammosphere formation, we cultured these cells with HRG in the absence of EGF, bFGF, or B27 supplement and then counted the number of mammospheres that formed. $CD44^{high}/CD24^{low}$/lineage$^-$ BCSC-enriched population cultured with HRG generated mammospheres at similar frequencies as those cultured with EGF/bFGF/B27, whereas $CD44^{low}/CD24^{high}$/lineage$^-$ nonstem cells did not generate mammospheres (Fig. 1 *A* and *B*). These findings suggest that HRG has the ability to induce mammosphere formation of BCSC-enriched population.

To further investigate the effect of HRG, we examined mammosphere formation in five breast cancer cell lines treated with HRG. Similar to the effects of HRG on primary human breast cancer cells, HRG increased mammosphere formation in four of the five breast cancer cell lines (Fig. 1 *C* and *D*) with an efficiency comparable to that of EGF. The HRG-induced mammospheres expressed the stem cell marker Nanog, comparable to mammospheres cultured with EGF/bFGF/B27 (Fig. 1*E*). Together, these results suggest that HRG plays an important role in enhancing the mammosphere formation of BCSC-enriched populations.

HRG Up-Regulates NF-κB Through PI3K/Akt Activation. To examine whether HRG treatment activates the ErbB2/ErbB3 pathway, we investigated the effect of HRG on the phosphorylation levels of ErbB2, ErbB3, ERK, and Akt in three breast cancer cell lines. HRG markedly induced the phosphorylation of ErbB2, ErbB3, ERK, and Akt (Fig. 2*A*) in all three cell lines, suggesting that HRG strongly activates ErbB2 and ErbB3, which leads to the activation of ERK and the PI3K/Akt pathway. To confirm that HRG promotes the interaction between ErbB2 and ErbB3, we performed an immunoprecipitation analysis after treatment with HRG. The analysis revealed that treatment with HRG led to increased interactions between ErbB3 and ErbB2 (Fig. 2*B*).

Because NF-κB is a downstream target of Akt, we investigated whether the NF-κB signaling pathway was also altered by HRG treatment. IKKα/β are the upstream kinases involved in the phosphorylation of IκBα, which leads to the nuclear translocation of NF-κB. Treatment with HRG markedly induced the phosphorylation of Akt and IKKα/β within 10 min and the phosphorylation of IκBα and the NF-κB subunit RELA after 30 min (Fig. 2*C*). To examine the DNA-binding activity of RELA after HRG stimulation, we quantified the intensity of the RELA/DNA complex by ELISA at various time intervals. Treatment with HRG induced a marked increase in the binding activity of RELA after 1 h, and then this activation gradually decreased until 4 h (Fig. 2*D*). To test whether the activation of RELA by HRG was dependent on the PI3K/Akt pathway, we pretreated cells with LY294002, an inhibitor of PI3K before the addition of HRG. As anticipated, the HRG-induced activation of NF-κB was completely inhibited by LY294002 in a manner similar to the inhibition after treatment with DHMEQ, a specific inhibitor of NF-κB (28) (Fig. 2*E* and Fig. S1). These results showed that NF-κB was activated by HRG through the PI3K/Akt pathway. Because our previous observations suggested that the NF-κB pathway is enriched in BCSCs (19), we speculated that the HRG/PI3K/Akt/NF-κB axis may have a role in regulating mammosphere formation.

HRG/PI3K/NF-κB Axis Controls Mammosphere Formation. To elucidate whether NF-κB or PI3K influences HRG-induced mammosphere formation, we treated MCF7 cells with HRG, together with DHMEQ or LY294002. Treatment with DHMEQ or LY294002 decreased the frequency of mammosphere formation in a dose-dependent manner (Fig. 3*A*); however, the sizes of the mammospheres were not significantly changed, suggesting that the activities of NF-κB or PI3K affect mammosphere initiation but do not primarily influence cell proliferation during mammosphere growth. To test secondary mammosphere formation, primary mammospheres generated in the presence of DHMEQ or LY294002 were dissociated into single cells and incubated with HRG in the absence of the inhibitors (Fig. 3*B*). We found that the cells derived from primary mammospheres formed in the presence of DHMEQ or LY294002 did not form secondary mammospheres as efficiently as cells from untreated mammospheres (Fig. 3 *C* and *D*). These findings suggest that the activities of NF-κB and PI3K are required to maintain mammosphere cells with the ability to initiate HRG-induced mammosphere formation. In agreement with these findings, we found that lapatinib, an inhibitor of EGF receptor and ErbB2 tyrosine kinases, decreased NF-κB activity and mammosphere formation (Fig. S2 and *SI Results*). To determine whether DHMEQ or LY294002 induces apoptosis, we stained mammosphere cells with propidium iodide (PI) following inhibitor treatments and then analyzed the cell-cycle status by flow cytometry (Fig. S3). There was no apparent sub-G1 cell population, indicating that

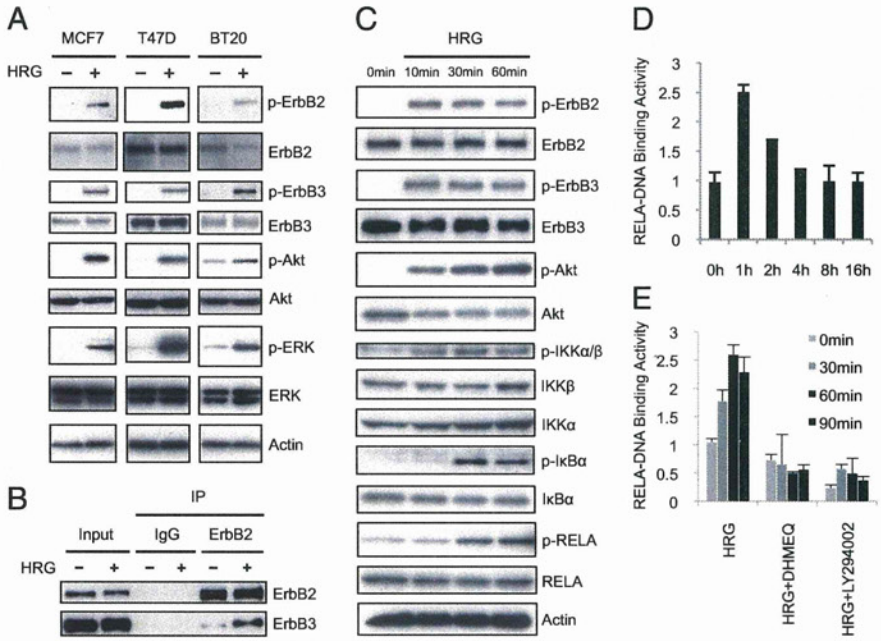

Fig. 2. HRG induces the ErbB/PI3K/Akt/NF-κB pathway. (*A*) MCF7, T47D, and BT20 cells were treated with 100 ng/mL HRG for 10 min, and protein expression levels were determined by immunoblotting. (*B*) MCF7 cells were treated with 100 ng/mL HRG for 10 min, and immunoprecipitation (IP) assays were performed with the indicated antibodies. (*C*) MCF7 cells were treated with 100 ng/mL HRG for 10, 30, and 60 min. Protein expression levels were determined by immunoblotting. (*D*) MCF7 cells were treated with 100 ng/mL HRG for 1, 2, 4, 8, and 16 h. The DNA binding activity of RELA was quantified by ELISA (data are mean ± SD; $n = 3$). (*E*) MCF7 cells were treated with 5 μg/mL DHMEQ (NF-κB inhibitor) or 10 μM LY294002 (PI3Kinase inhibitor) for 2 h, and then the cells were treated with 100 ng/mL HRG for 30, 60, and 90 min. The DNA-binding activity of RELA was quantified by ELISA (data are mean ± SD; $n = 3$).

the inhibitors did not induce apoptosis at the effective concentrations for mammosphere formation.

NF-κB Is Required to Maintain Mammosphere-Forming Ability and Tumorigenic Potential of MCF7 Breast Cancer Cells. To further validate these findings, we overexpressed mutant IκBα (IκBαSR), a dominant-negative inhibitor of NF-κB, in MCF7 cells with a lentiviral vector. Overexpression of mutant IκBα resulted in a decrease in the number of HRG-induced mammospheres compared with the vector-transduced cells (Fig. 3*E*). We also attempted to determine whether NF-κB regulates the mammosphere-forming ability in culture containing EGF/bFGF/B27, and found that NF-κB activity was required for mammosphere formation in such a culture condition. These results suggest that NF-κB is a mediator of mammosphere-forming capacity in both HRG- and EGF/bFGF/B27-containing media (Figs. S4 and S5 and *SI Results*).

To test whether the down-regulation of NF-κB signaling alters the tumor-initiating ability in vivo, we injected 1×10^5 MCF7 cells constitutively expressing mutant IκBα into the mammary fat pads of NOD/SCID mice. There were no significant morphological differences between these cells and control cells in culture (Fig. S6, *Upper*). All eight mice injected with control cells developed tumors within 6 wk, whereas tumor formation was inefficient in the mice injected with cells expressing mutant IκBα (four of eight mice) (Fig. 3*F*). Histological analysis showed that tumors derived from the vector-transduced cells or IκBαSR-transduced cells had a similar morphology (Fig. S6, *Lower*). Therefore, it is unlikely that the reduced incidence of tumor formation by expression of IκBαSR is due to cell differentiation; rather, it appears that NF-κB activity is required for tumor initiation of MCF7 cells in vivo.

By extension, we speculated that an NF-κB-negative subpopulation could not generate mammospheres. To isolate living cells based on NF-κB activity, we used an NF-κB reporter lentiviral vector expressing d2Venus (a yellow fluorescent protein) driven by four copies of the NF-κB response element located upstream of the minimal TATA promoter. We isolated MCF7 cells expressing d2Venus at high ($NFkB^+$) or low ($NFkB^-$) levels (Fig. 3*G*); the activity of NF-κB is thought to be higher in the former cells than in the latter cells. As expected, the NF-κB–negative subpopulation showed significantly decreased mammosphere formation capacity compared with the NF-κB–positive subpopulation (Fig. 3*H*). Taken together, these in vitro and in vivo results showed that NF-κB is required for mammosphere formation and tumor initiation of MCF7 cells.

HRG Elicits PI3K/NF-κB–Dependent Up-Regulation of IL8 mRNA Expression. IL8 signaling has been shown to play a role in BCSC self-renewal (29, 30). Because the expression of *IL8* is regulated by NF-κB activity (31), we investigated whether HRG induces the expression of *IL8*. We also examined the expression of representative immediate early genes, *c-Fos* and *c-Myc*. Treatment with HRG resulted in a dramatic increase of *IL8* expression (up to a 100-fold increase) after 2 h (Fig. 4 *A* and *B*). The expression levels of *c-Fos* and *c-Myc* were also increased (10-fold and five-fold, respectively) (Fig. 4 *A* and *B*). The levels of these mRNAs were decreased rapidly after 4 h. To determine whether the activity of NF-κB or PI3K is involved in the induction of *IL8* expression by HRG, cells were stimulated with HRG in the presence of DHMEQ or LY294002. We found that the levels of *IL8* induction by HRG were decreased by treatment with inhibitors, although the induction levels of *c-Fos* or *c-Myc* were not significantly changed (Fig. 4 *A* and *B*). These results suggest that the expression of *IL8* is induced by the HRG/PI3K/NF-κB axis.

HRG/PI3K/NF-κB Axis Controls Mammosphere Formation of Primary Tumor Cells Derived from Breast Cancer Patients. We extended our analyses to primary tumor cells isolated directly from human breast cancer tissues (Table S1). To assess the effect of HRG,

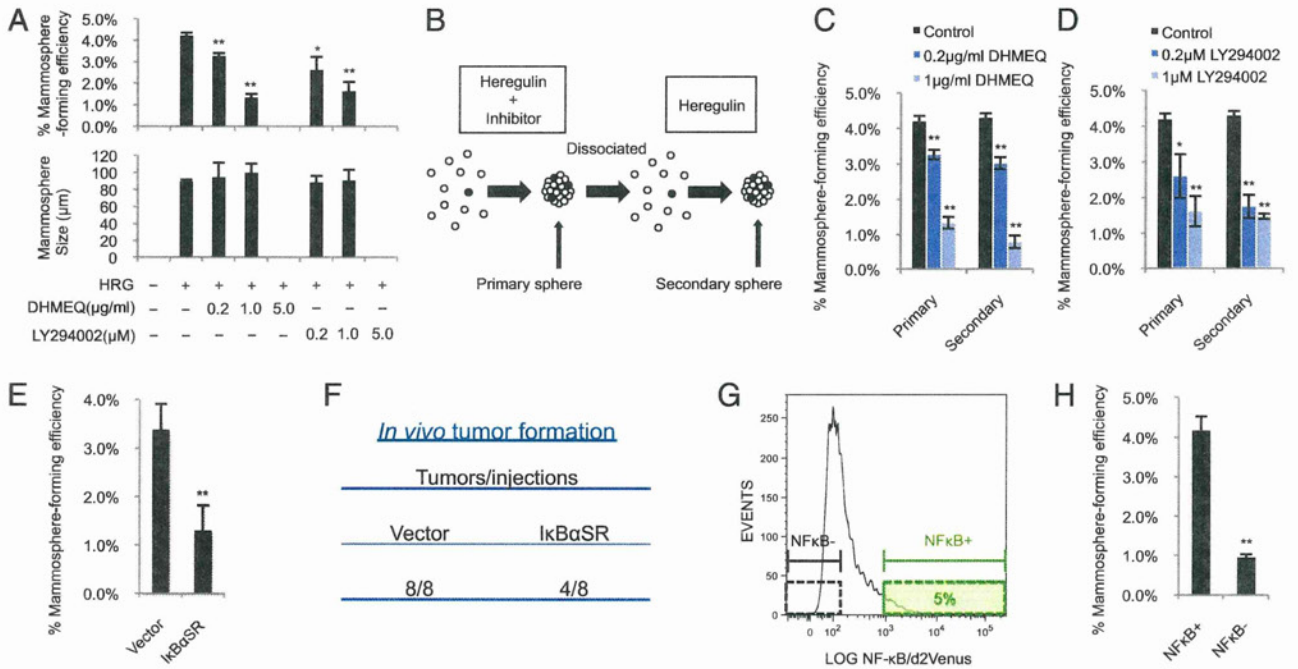

Fig. 3. Role of the HRG/PI3K/NF-κB axis on mammosphere formation. (*A*) MCF7 cells were incubated with 20 ng/mL HRG and/or the indicated concentrations of DHMEQ and LY294002. The number of formed mammospheres was counted, and the percentage of mammosphere-forming cells was determined [data are mean ± SD; $n = 3$, $^{**}P < 0.01$, $^{*}P < 0.05$, relative to the values in the HRG(+)]. (*B*) Experimental strategies for evaluating the effect of initial treatment with inhibitors on secondary mammosphere formation. (*C* and *D*) Effects of DHMEQ and LY294002 on primary and secondary mammosphere formation. MCF7 cells were incubated with 20 ng/mL HRG and/or the indicated concentrations of DHMEQ and LY294002. The formed primary mammospheres were dissociated into single cells and grown as secondary mammospheres without treatment with inhibitors. The mammospheres were counted, and the percentage of mammosphere-forming cells was determined (data are mean ± SD; $n = 3$, $^{**}P < 0.01$, $^{*}P < 0.05$, relative to the values in the respective controls). (*E*) MCF7 cells expressing the indicated lentiviral vectors were incubated with 20 ng/mL HRG, and the percentage of mammosphere-forming cells was determined (data are mean ± SD; $n = 4$, $^{**}P < 0.01$). (*F*) NOD/SCID mice were injected in the mammary fat pad with 1×10^5 of vector- or IκBαSR-transduced MCF7 cells. Tumor formation was indicated by tumors/injections at 6 wk after injection. (*G*) NF-κB reporter activity of mammospheres derived from MCF7 cells. (*H*) NF-κB$^+$ cells and NF-κB$^-$ cells (Fig. 3*G*) were sorted by FACS and cultured with 20 ng/mL HRG. The percentage of mammosphere-forming cells was determined (data are mean ± SD; $n = 4$, $^{**}P < 0.01$).

PI3K, and NF-κB on mammosphere formation, primary tumor cells were treated with HRG, together with DHMEQ or LY294002. Treatment with HRG induced mammosphere formation in all tumor samples, and the effect of HRG was blocked when DHMEQ or LY294002 was added with HRG (Fig. 5*A* and *B*). We confirmed that both ErbB2 and ErbB3 were expressed in these cells and that the phosphorylation of Akt and IκBα was induced in response to HRG (Fig. 5*C*). When we treated primary tumor cells with HRG, together with LY294002, the phosphorylation levels of Akt and IκBα were decreased, suggesting that NF-κB was activated by HRG through the PI3K/Akt pathway in primary tumor cells. (Fig. S1). Furthermore, overexpression of mutant IκBα in primary tumors cells with a lentiviral vector led to a decreased frequency of mammosphere formation compared with the control vector–transduced cells (Fig. 5*D*). Similar results were obtained in mammospheres cultured with EGF/bFGF/B27 (Fig. 5*D* and Fig. S7 *A* and *B*). These results suggest that the mammosphere formation of primary tumor cells derived from breast cancer patients is regulated by the HRG/PI3K/NF-κB pathway, which is consistent with the results obtained from the analysis performed with breast cancer cell lines.

Discussion

Accumulating evidence indicates that BCSCs are responsible for the initiation, propagation, recurrence, and radioresistance of breast cancers (1, 15, 32); hence, BCSCs are considered to be critical therapeutic targets (30, 33, 34). Recent studies have indicated that BCSC-enriched populations give rise to mammospheres in anchorage-independent conditions (11, 12). An understanding of the molecular mechanisms involved in the regulation of mammosphere formation is important for the design of efficient therapeutic strategies and improvements in conventional anticancer treatments. Recently, several inflammatory chemokines have been found to play a role in regulating the mammosphere-forming ability of breast cancer cells (18). However, the molecular pathways linking inflammation to mammosphere-forming ability are still largely unknown. In the present study, we describe one such molecular pathway that involves HRG, PI3K/Akt, NF-κB, and IL8.

HRG is widely expressed in numerous tissues, including breast, brain, heart, skeletal muscle, liver, and lung, and it is implicated in the regulation of a variety of biological processes, including cell proliferation, apoptosis and differentiation (35). We have identified yet another role of HRG in human breast cancer: induction of the mammosphere-forming capacity of BCSC-enriched populations. We demonstrated that the effects of HRG on mammosphere formation are mediated through a PI3K/NF-κB pathway in breast cancer cell lines and primary tumor cells derived from surgically resected breast cancer tissues. The first step of HRG stimulation is activation of PI3K, followed by the phosphorylation of Akt, which occurs within 10 min after treatment with HRG. Activated Akt phosphorylates IKKα/β and then leads to phosphorylation of IκBα, resulting in NF-κB activation. Once the signal has been activated, production of IL8 is induced at high levels. IL8 increases the self-renewal capacity of BCSC-enriched populations through nuclear translocation of β-catenin (36), indicating that the HRG/NF-κB pathway-mediated initiation of

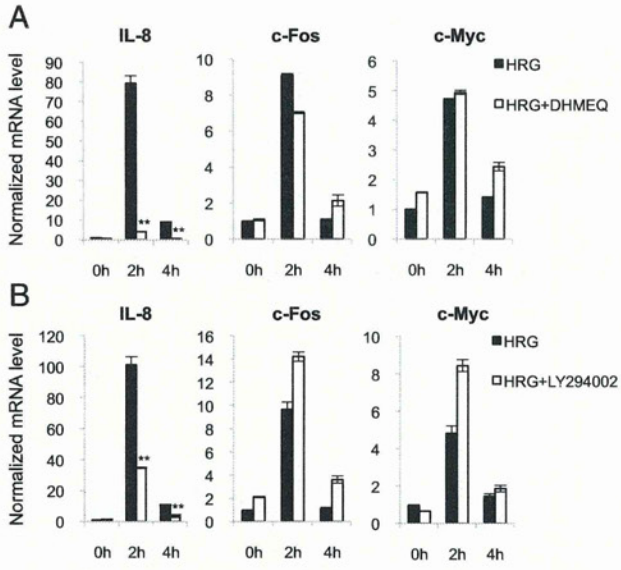

Fig. 4. IL8 is a transcriptional target of NF-κB. (*A* and *B*) MCF7 cells were treated with 5 μg/mL DHMEQ or 5 μM LY294002 for 2 hours, and then the cells were treated with 100 ng/mL HRG for 2 h and 4 h. Expression levels of *IL8*, *c-Fos*, and *c-Myc* were examined by quantitative RT-PCR (data are mean ± SD; $n = 3$, $^{**}P < 0.01$, relative to the values in the respective controls).

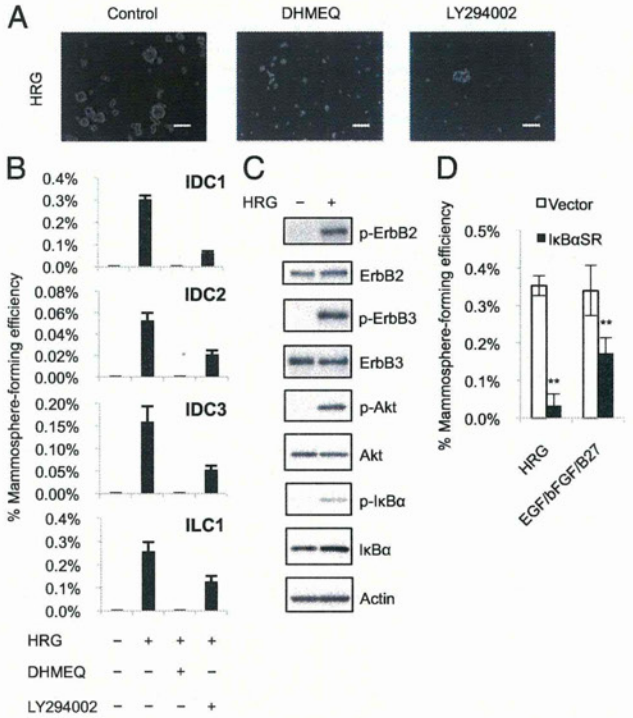

Fig. 5. The HRG/PI3K/NF-κB axis controls mammosphere formation of primary tumor cells derived from breast cancer patients. (*A*) Representative images of primary cultures of mammospheres incubated with 20 ng/mL HRG, 5 μg/mL DHMEQ and 5 μM LY294002. Scale bar = 100 μm. (*B*) Primary breast cancer cells obtained from specimens of invasive ductal carcinoma (IDC1, 2, and 3) or invasive lobular carcinoma (ILC1) were treated as indicated in *A*, and the percentage of mammosphere-forming cells was determined (data are mean ± SD; $n = 4$). (*C*) Cells from IDC1 were incubated with 100 ng/mL HRG for 10 min, and protein expression levels were determined by immunoblotting. (*D*) Cells from IDC1 expressing the indicated lentiviral vectors were incubated with 20 ng/mL HRG or with EGF/bFGF/B27, and the percentage of mammosphere-forming cells was determined (data are mean ± SD; $n = 4$, $^{**}P < 0.01$, relative to the values in the respective controls).

mammosphere formation is regulated by this pathway, at least in part. Together, these observations suggest a tight link between the HRG-induced mammosphere formation and the NF-κB–dependent inflammatory signaling pathway.

NF-κB is a central regulator of inflammatory gene expression (37). The findings presented here describe an important role of NF-κB in regulating mammosphere formation. NF-κB was activated by HRG stimulation as well as by culture with EGF/bFGF/B27, and it regulated the mammosphere formation under each culture condition. Down-regulation of NF-κB led to a decreased frequency of tumor initiation of MCF7 cells and mammosphere formation, and the cells that had low NF-κB activity showed a decreased frequency of mammosphere formation. These observations suggest that NF-κB activity is required to maintain the mammosphere-forming ability of breast cancer cells.

ErbB3 is the only ErbB family member that directly binds to PI3K (38). As ErbB3 has six direct binding sites for p85, a subunit of PI3K, the signaling output of ErbB3 is dominated by activation of the PI3K cascade, leading to activation of Akt. Although ErbB3 lacks intrinsic kinase activity, it is well known that ErbB family members homodimerize or heterodimerize to activate signaling pathways. Among the various combinations of family members, the ErbB2/ErbB3 heterodimer is considered the most potent ErbB pair with respect to the strength of interaction, ligand-induced tyrosine phosphorylation, and downstream signaling (39). Because there is no ligand for ErbB2, HRG is among the most efficient ligands to activate ErbB2/ErbB3 heterodimers. This could be the reason why HRG stimulates strong activation of the PI3K/NF-κB pathway for the mammosphere formation of breast cancer cells.

Trastuzumab (Herceptin, Genentech), a humanized monoclonal antibody directed at the ErbB2 ectodomain, is effective in the treatment of some human breast cancers that overexpress ErbB2 (40). In this study, we showed that the HRG signaling pathway plays important roles for mammosphere formation in primary tumor cells derived from human breast cancer tissues in which ErbB2 was expressed at moderate levels (Table S1) as well as in breast cancer cell lines in which ErbB2 was expressed at various levels. This raises the intriguing possibility that trastuzumab effectively targets BCSCs in the breast cancer tissues in which HRG is overexpressed even if ErbB2 is expressed at moderate levels. Indeed, it was recently reported that trastuzumab sensitizes HRG-overexpressing breast cancer cells to chemotherapy (23).

In conclusion, our results suggest that HRG/ErbB/PI3K/NF-κB signaling regulates the mammosphere formation of human breast cancer cells. Hence, in the future it will be important to develop compounds or antibodies targeted at the signaling molecules involved in this pathway to improve the prognosis of breast cancer patients.

Materials and Methods

Cell Lines and Primary Cell Culture. Breast cancer cell lines MCF7, T47D, BT20 HCC1954, and HCC1143 were purchased from the American Type Culture Collection (ATCC). Cells were cultured in RPMI1640 with 10% (vol/vol) FBS. Primary cultures of tumor cells and mammospheres were generated as described previously (12–14). Briefly, tumor samples were processed within 1 h after surgical resection. Minced pieces of human breast tumor samples were digested with 2 mg/mL collagenase A (Roche), 1 mM $CaCl_2$, and DNaseI (Roche) in RPMI1640 with 10% FBS. Tumors were digested for 1.5–2.5 h at 37 °C with shaking and pipetting every 30 min for mechanical dissociation. Once tumors were digested, the resulting single-cell suspension was filtered through a 100-μm and 40-μm cell strainer (BD Falcon) and washed with PBS. After isolation of lineage-negative (Lin^-) breast cancer cells, cells were cultured in human mammary epithelial cell growth medium (HuMEC, GIBCO) or in mammosphere culture medium, which consisted of serum-free Dulbecco's modified Eagle's Medium:Nutrient

Mixture F-12 (DMEM/F-12) medium (GIBCO) supplemented with 20 ng/mL EGF (Millipore), 20 ng/mL bFGF (PeproTech), B27 (GIBCO), and heparin (Stem Cell Technologies). B27 supplement has been shown to support the growth of mammospheres from human breast tissue (41). Alternatively, mammospheres were grown in DMEM/F12 medium supplemented with 20 ng/mL HRG-β1 (R&D).

Human breast carcinoma specimens were obtained from the University of Tokyo Hospital and Showa General Hospital. This study was approved by the institutional review boards of the Institute of Medical Science, University of Tokyo, and Showa General Hospital.

Cell Isolation. To isolate Lin^- breast cancer cells, cells obtained from breast tumor specimens were incubated with a mixture of biotin-conjugated antibodies against Lin^+ cells. The mixture of antibodies included a MACS lineage depletion kit for hematopoietic and erythrocyte precursor cells (CD2, CD3, CD11b, CD14, CD15, CD16, CD19, CD56, CD123, and CD235a, Miltenyi Biotec), CD31 (for endothelial cells, eBioscience) and CD140b (for stromal cells, Biolegend) antibody. After incubation, cells were separated using the MACS magnetic cell separation system according to the manufacturer's instructions (Miltenyi Biotec). To isolate putative stem cells, Lin^- breast cancer cells were then sorted after staining with CD24-FITC or CD44-PE antibody (BD Pharmingen) using a FACSAria Cell Sorter (BD Bioscience). Dead cells were excluded by propidium iodide (PI, Sigma) staining. Data were analyzed by FlowJo software.

Mammosphere Assay. Cells were plated as single cells in ultralow attachment plates at a low density (5,000 cells/mL) and were grown in mammosphere culture medium with or without NF-κB inhibitor DHMEQ (28), PI3K inhibitor LY294002 (Cell Signaling), lapatinib (Selleck Chemicals), gefitinib (AstraZeneca), dasatinib (Selleck Chemicals), or sunitinib (Sigma-Aldrich) at the indicated concentrations for 4–7 d. To test whether the low-density conditions, such as 5,000 cells/mL, represented clonal expansion rather than aggregation, as previously reported (11), we performed mammosphere assays using primary tumor cells from patients under the condition of 50 cells/well in 96-well plates (*SI Materials and Methods*). We found a comparable frequency of mammosphere formation irrespective of cell-plating density, strongly suggesting that mammospheres are not formed by simple cell aggregation but by clonal expansion of single cells. To culture secondary mammospheres, primary mammospheres were collected by gentle centrifugation (400 × *g*), and cells were dissociated enzymatically and mechanically into a single-cell suspension. The single-cell suspension was replated as described above.

Statistical Analysis. All data were presented as mean ± SD. The unpaired Student *t* test was used for the statistical analysis. *P* values less than 0.05 were considered statistically significant.

ACKNOWLEDGMENTS. We thank H. Nakauchi and Y. Ishii for their help with flow cytometry, N. Yamaguchi for preparing the IκBαSR construct, N. Haraguchi for advising on the design of the in vivo experiments, T. Haraguchi for advising on the generation of the lentiviruses, and Y. Murakami, H. Kawahara and M. Kuroda for preparing the H&E sections. This work was supported by a grant from the Ministry of Health, Labor and Welfare of Japan for the Third Term Comprehensive 10-Year Strategy for Cancer Control; by a Grant-in-Aid from the Ministry of Education, Science, Sports and Culture of Japan for Scientific Research on Innovative Areas; and by grants from the Cell Science Research Foundation.

1. Reya T, Morrison SJ, Clarke MF, Weissman IL (2001) Stem cells, cancer, and cancer stem cells. *Nature* 414:105–111.
2. Gotoh N (2011) Potential signaling pathways activated in cancer stem cells in breast cancer. *Cancer Stem Cells Theories and Practice*, ed Shostak S (InTech, Vienna, Austria), p 6.
3. Al-Hajj M, Wicha MS, Benito-Hernandez A, Morrison SJ, Clarke MF (2003) Prospective identification of tumorigenic breast cancer cells. *Proc Natl Acad Sci USA* 100: 3983–3988.
4. Boiko AD, et al. (2010) Human melanoma-initiating cells express neural crest nerve growth factor receptor CD271. *Nature* 466:133–137.
5. Bonnet D, Dick JE (1997) Human acute myeloid leukemia is organized as a hierarchy that originates from a primitive hematopoietic cell. *Nat Med* 3:730–737.
6. Chan KS, et al. (2009) Identification, molecular characterization, clinical prognosis, and therapeutic targeting of human bladder tumor-initiating cells. *Proc Natl Acad Sci USA* 106:14016–14021.
7. Dalerba P, et al. (2007) Phenotypic characterization of human colorectal cancer stem cells. *Proc Natl Acad Sci USA* 104:10158–10163.
8. O'Brien CA, Pollett A, Gallinger S, Dick JE (2007) A human colon cancer cell capable of initiating tumour growth in immunodeficient mice. *Nature* 445:106–110.
9. Prince ME, et al. (2007) Identification of a subpopulation of cells with cancer stem cell properties in head and neck squamous cell carcinoma. *Proc Natl Acad Sci USA* 104: 973–978.
10. Singh SK, et al. (2003) Identification of a cancer stem cell in human brain tumors. *Cancer Res* 63:5821–5828.
11. Cordenonsi M, et al. (2011) The Hippo transducer TAZ confers cancer stem cell-related traits on breast cancer cells. *Cell* 147:759–772.
12. Pece S, et al. (2010) Biological and molecular heterogeneity of breast cancers correlates with their cancer stem cell content. *Cell* 140:62–73.
13. Dontu G, et al. (2003) In vitro propagation and transcriptional profiling of human mammary stem/progenitor cells. *Genes Dev* 17:1253–1270.
14. Ponti D, et al. (2005) Isolation and in vitro propagation of tumorigenic breast cancer cells with stem/progenitor cell properties. *Cancer Res* 65:5506–5511.
15. Yu F, et al. (2007) let-7 Regulates self renewal and tumorigenicity of breast cancer cells. *Cell* 131:1109–1123.
16. Scheel C, et al. (2011) Paracrine and autocrine signals induce and maintain mesenchymal and stem cell states in the breast. *Cell* 145:926–940.
17. Hsing CH, et al. (2011) Anesthetic propofol reduces endotoxic inflammation by inhibiting reactive oxygen species-regulated Akt/IKKβ/NF-κB signaling. *PLoS ONE* 6: e17598.
18. Hinohara K, Gotoh N (2010) Inflammatory signaling pathways in self-renewing breast cancer stem cells. *Curr Opin Pharmacol* 10:650–654.
19. Murohashi M, et al. (2010) Gene set enrichment analysis provides insight into novel signalling pathways in breast cancer stem cells. *Br J Cancer* 102:206–212.
20. Hayes NV, Gullick WJ (2008) The neuregulin family of genes and their multiple splice variants in breast cancer. *J Mammary Gland Biol Neoplasia* 13:205–214.
21. Krane IM, Leder P (1996) NDF/heregulin induces persistence of terminal end buds and adenocarcinomas in the mammary glands of transgenic mice. *Oncogene* 12: 1781–1788.
22. Atlas E, et al. (2003) Heregulin is sufficient for the promotion of tumorigenicity and metastasis of breast cancer cells in vivo. *Mol Cancer Res* 1:165–175.
23. Menendez JA, Mehmi I, Lupu R (2006) Trastuzumab in combination with heregulin-activated Her-2 (erbB-2) triggers a receptor-enhanced chemosensitivity effect in the absence of Her-2 overexpression. *J Clin Oncol* 24:3735–3746.
24. Dunn M, et al. (2004) Co-expression of neuregulins 1, 2, 3 and 4 in human breast cancer. *J Pathol* 203:672–680.
25. Korkaya H, Paulson A, Iovino F, Wicha MS (2008) HER2 regulates the mammary stem/progenitor cell population driving tumorigenesis and invasion. *Oncogene* 27: 6120–6130.
26. Ginestier C, et al. (2007) ALDH1 is a marker of normal and malignant human mammary stem cells and a predictor of poor clinical outcome. *Cell Stem Cell* 1:555–567.
27. Mani SA, et al. (2008) The epithelial-mesenchymal transition generates cells with properties of stem cells. *Cell* 133:704–715.
28. Nishimura D, et al. (2006) DHMEQ, a novel NF-kappaB inhibitor, induces apoptosis and cell-cycle arrest in human hepatoma cells. *Int J Oncol* 29:713–719.
29. Charafe-Jauffret E, et al. (2009) Breast cancer cell lines contain functional cancer stem cells with metastatic capacity and a distinct molecular signature. *Cancer Res* 69: 1302–1313.
30. Ginestier C, et al. (2010) CXCR1 blockade selectively targets human breast cancer stem cells in vitro and in xenografts. *J Clin Invest* 120:485–497.
31. Pahl HL (1999) Activators and target genes of Rel/NF-kappaB transcription factors. *Oncogene* 18:6853–6866.
32. Diehn M, et al. (2009) Association of reactive oxygen species levels and radioresistance in cancer stem cells. *Nature* 458:780–783.
33. Gupta PB, et al. (2009) Identification of selective inhibitors of cancer stem cells by high-throughput screening. *Cell* 138:645–659.
34. Morrison BJ, Schmidt CW, Lakhani SR, Reynolds BA, Lopez JA (2008) Breast cancer stem cells: Implications for therapy of breast cancer. *Breast Cancer Res* 10:210.
35. Stove C, Bracke M (2004) Roles for neuregulins in human cancer. *Clin Exp Metastasis* 21:665–684.
36. Liu S, Wicha MS (2010) Targeting breast cancer stem cells. *J Clin Oncol* 28:4006–4012.
37. Karin M, Greten FR (2005) NF-kappaB: Linking inflammation and immunity to cancer development and progression. *Nat Rev Immunol* 5:749–759.
38. Hynes NE, Lane HA (2005) ERBB receptors and cancer: The complexity of targeted inhibitors. *Nat Rev Cancer* 5:341–354.
39. Olayioye MA, Neve RM, Lane HA, Hynes NE (2000) The ErbB signaling network: Receptor heterodimerization in development and cancer. *EMBO J* 19:3159–3167.
40. Vogel CL, et al. (2002) Efficacy and safety of trastuzumab as a single agent in first-line treatment of HER2-overexpressing metastatic breast cancer. *J Clin Oncol* 20:719–726.
41. Lim E, et al.; kConFab (2009) Aberrant luminal progenitors as the candidate target population for basal tumor development in BRCA1 mutation carriers. *Nat Med* 15: 907–913.

Supporting Information

Hinohara et al. 10.1073/pnas.1113271109

SI Results

Effects of Tyrosine Kinase Inhibitors on NF-κB Activity and Mammosphere Formation. We assessed the effects of tyrosine kinase inhibitors on the NF-κB activity and mammosphere-forming ability of MCF7 cells. The following tyrosine kinase inhibitors were used: lapatinib, which inhibits EGF receptor (EGFR) and ErbB2; gefitinib, which inhibits EGFR; dasatinib, which inhibits Src; and sunitinib. We treated MCF7 cells with HRG together with these inhibitors. Treatment with lapatinib decreased NF-κB activity and mammosphere formation, whereas the other tyrosine kinase inhibitors did not significantly affect NF-κB activity and mammosphere formation (Fig. S2 *A* and *B*). DHMEQ plus lapatinib had an additive effect on the inhibition of mammosphere formation (Fig. S2*C*).

NF-κB Regulates Mammosphere Formation in EGF/bFGF/B27-Containing Medium. Treatment with EGF/bFGF/B27 did not significantly induce phosphorylation of ErbB2/ErbB3, but it did induce strong phosphorylation of the FGF receptor substrate 2α (FRS2α), a membrane-anchored docking protein involved in FGF signaling (Fig. S4*A*) (1, 2). Furthermore, bFGF but not EGF increased mammosphere formation (Fig. S4*B*), suggesting that MCF7 mammosphere growth in the presence of EGF/bFGF/B27 is dependent on bFGF rather than EGF. Consistent with this result, the expression level of EGFR was low in MCF7 cells (Fig. S4*A*). Compared with adherent cells, we found that the NF-κB activities were higher in mammosphere cells cultured with EGF/bFGF/B27 (Fig. S5*A*). We then cultured mammospheres in the presence of DHMEQ with EGF/bFGF/B27. Treatment with DHMEQ decreased the number of both primary and secondary mammospheres (Fig. S5*B*). In addition, the expression of the IκBα mutant resulted in a decreased frequency of mammosphere formation during serial passages (Fig. S5*C*). These results further support the role of NF-κB in regulating mammosphere formation.

SI Materials and Methods

Mammosphere Assay Performed with Different Cell-Plating Densities. We performed mammosphere assays with primary tumor cells from breast cancer patients. Cells were plated at the density of 5,000 cells/mL in six-well plates or 50 cells/100 μL per well in 96-well plates (500 cells/mL). If the mammospheres were derived from clonal expansion of single cells rather than aggregation, the frequencies of mammosphere formation were expected to be fairly constant irrespective of cell-plating density. Under conditions of 50 cells per well, we observed only single mammospheres in 19.0 ± 1.0 wells and 17.3 ± 1.5 wells per 96-well plate when cultured with EGF/bFGF/B27 or HRG, respectively. Because each well contained only one mammosphere, this result yielded mammosphere-forming frequencies of 0.40% ± 0.02% and 0.36% ± 0.03% when cultured with EGF/bFGF/B27 or HRG, respectively. When tumor cells from the same patient were plated at 5,000 cells/mL, the mammosphere-forming frequencies were 0.37% ± 0.04% in the presence of EGF/bFGF/B27 and 0.30% ± 0.02% in the presence of HRG. These data suggest that the mammospheres cultured at densities of 5,000 cells/mL or less are clonally derived from single cells. This result is consistent with the previous report (3).

Xenografts. Eight-week-old female NOD/SICD mice were anesthetized with isoflurane (Abbott Japan), and 60 d-release β-estradiol (E2) pellets containing 0.72 mg of E2 (Innovative Research of America) were s.c. implanted on the back of the neck. A total of 1×10^5 MCF7 cells expressing the indicated constructs were suspended in 1:1 volumes of PBS (PBS)/Matrigel (BD Biosciences) to produce 100 μL of the cell mixture that was subsequently injected into the mammary fat pads.

Construction of Lentiviral Vectors. Plasmids containing cDNA encoding mutant IκBα (IκBαSR) were cloned into a CSII-EF-MCS-IRES2-Venus vector that was a kind gift from H. Miyoshi (RIKEN, Tsukuba, Japan) by standard molecular biological techniques (4). The CSII-EF-MCS-IRES2-Venus vector is a plasmid with a gene encoding d2Venus (5) (provided by A. Miyawaki, RIKEN, Wako, Japan). Viral supernatant was produced by cotransfecting CSII-EF-MCS-IRES2-Venus vector with packaging plasmid pCMV-VSV-G-RSV-Rev and pCAG-HIVgp in 293T cells by using lipofectamine (Invitrogen), as previously described (6). The viral titers were determined by transducing HeLa cells at serial dilutions and analyzed by the amount of integrated DNA measured by the quantitative real-time PCR method (DNA titer). High-titer viral stocks were prepared by ultracentrifugation.

Transduction of Cells with Lentiviral Vectors. Cells were pelleted and infected with viral supernatant containing 5 μg/mL polybrene (Millipore) at a multiplicity of infection of 1:10 and then incubated for 3 h at 37 °C in 5% CO_2.

Immunoblot Analysis and Immunoprecipitation. Western blotting was performed by standard procedures. All antibodies were purchased from Cell Signaling Technology and used at a 1:1,000 dilution, unless otherwise noted. Antibodies against the following proteins were used: ErbB2, p-ErbB2, ErbB3, p-ErbB3, Akt, p-Akt, Erk1/2, p-Erk1/2, IKKα, IKKβ, p-IKKα/β, IκBα, p-IκBα, RELA (1:2,000 dilution), p-RELA, FRS2α (1:100 dilution; Santa Cruz), p-FRS2α, and actin (1:5,000 dilution; Millipore). For immunoprecipitation, cell lysates were precleared with protein G–Sepharose beads (GE Healthcare) for 1h and then incubated for 1 h on ice with rabbit monoclonal antibody to ErbB2, after which protein G–Sepharose beads were added and the mixture was incubated for an additional 1 h. The beads were isolated by centrifugation and washed three times with lysis buffer, after which the bead-bound proteins were subjected to immunoblot analysis.

Quantification of NF-κB Activity. Nuclear extracts were prepared with a Nuclear Extract kit (Active Motif), and NF-κB RELA-DNA binding activity was measured with a TransAM NF-κB p65 Transcription Factor Assay kit (Active Motif) according to the manufacturer's protocol.

Quantitative Real-Time PCR. Total RNA was prepared by using TRIzol Reagent (Invitrogen) and then transcribed into cDNA with a High Capacity cDNA Reverse Transcription kit (Applied Biosystems). Quantitative RT-PCR was performed with Taqman probes from Applied Biosystems, according to the manufacturer's recommendations. Reactions were performed in an Applied Biosystems StepOne real-time PCR system.

Cell-Cycle Analysis. Mammosphere cells were fixed in 70% ethanol for 2 h at 4 °C. They were washed twice with PBS, followed by RNase treatment (0.25 mg/mL) and PI (50 μg/mL) staining for 15 min at 37 °C in the dark. Cell-cycle analysis was performed by using a FACSAria Cell Sorter (BD Bioscience).

1. Eswarakumar VP, Lax I, Schlessinger J (2005) Cellular signaling by fibroblast growth factor receptors. *Cytokine Growth Factor Rev* 16:139–149.
2. Gotoh N (2008) Regulation of growth factor signaling by FRS2 family docking/scaffold adaptor proteins. *Cancer Sci* 99:1319–1325.
3. Pece S, et al. (2010) Biological and molecular heterogeneity of breast cancers correlates with their cancer stem cell content. *Cell* 140:62–73.
4. Miyoshi H, Smith KA, Mosier DE, Verma IM, Torbett BE (1999) Transduction of human CD34+ cells that mediate long-term engraftment of NOD/SCID mice by HIV vectors. *Science* 283:682–686.
5. Nagai T, et al. (2002) A variant of yellow fluorescent protein with fast and efficient maturation for cell-biological applications. *Nat Biotechnol* 20:87–90.
6. Murohashi M, et al. (2010) Gene set enrichment analysis provides insight into novel signalling pathways in breast cancer stem cells. *Br J Cancer* 102:206–212.

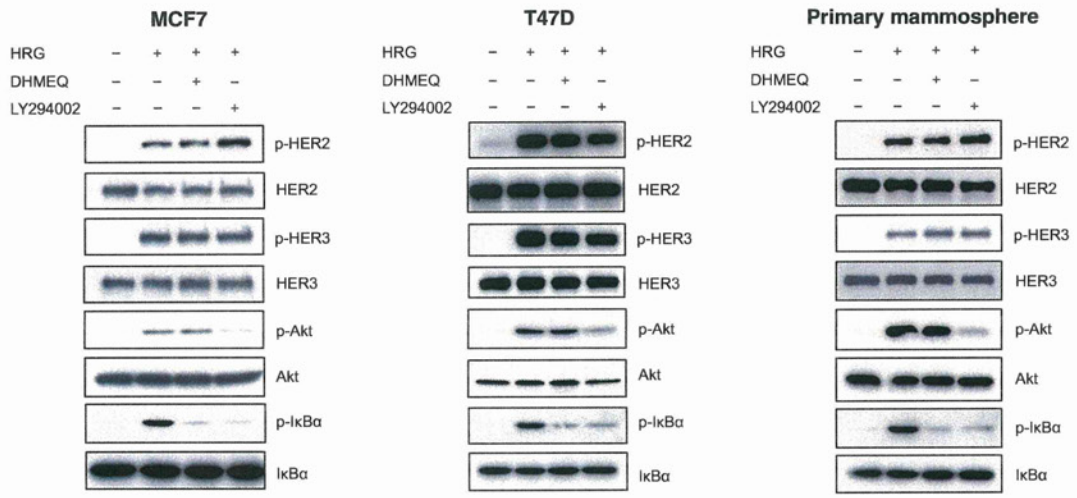

Fig. S1. Effect of DHMEQ and LY294002 on phosphorylation of Akt and IκBα. MCF7, T47D, and primary mammosphere cells were treated with 5 μg/mL DHMEQ (NF-κB inhibitor) or 5 μM LY294002 (PI3K inhibitor) for 1 h, and then the cells were treated with 100 ng/mL HRG for 30 min. The levels of p-ErbB2, ErbB2, p-ErbB3, ErbB3, p-Akt, Akt, p-IκBα, and IκBα were determined by immunoblotting. DHMEQ decreased the phosphorylation of IκBα, whereas LY294002 inhibited the phosphorylation of both Akt and IκBα.

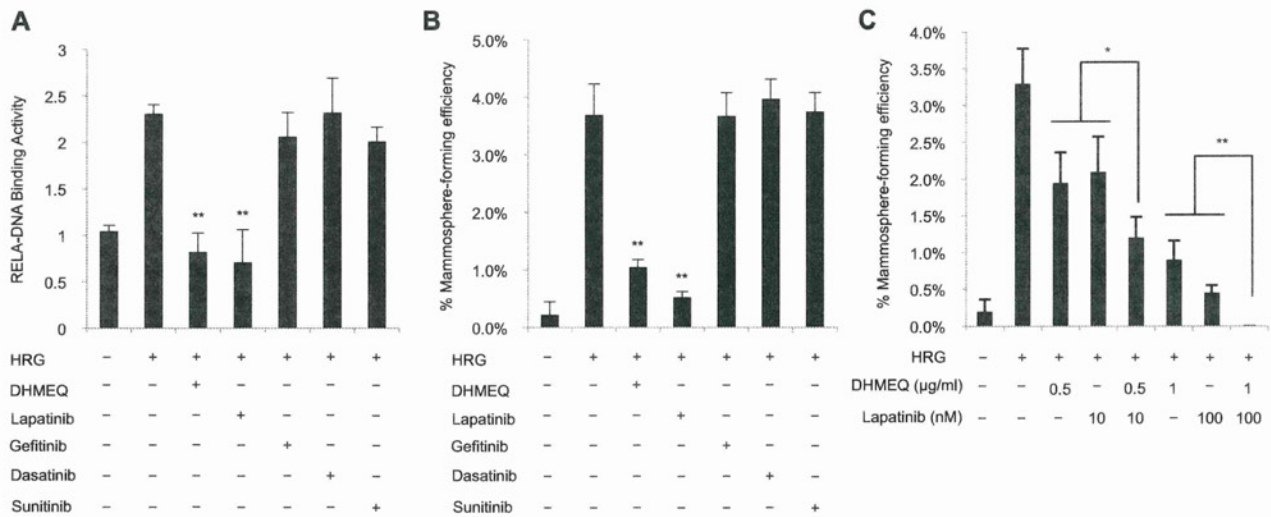

Fig. S2. Effect of tyrosine kinase inhibitors on mammosphere formation and NF-κB activity. (*A*) MCF7 cells were treated with 1 μg/mL DHMEQ, 100 nM lapatinib, 100 nM gefitinib, 100 nM dasatinib, and 100 nM sunitinib for 1 h, and then the cells were treated with 100 ng/mL HRG for 1 h. The DNA-binding activity of RELA was quantified by ELISA [data are mean ± SD; $n = 3$, $^{**}P < 0.01$, relative to the values in the HRG(+)]. (*B*) MCF7 cells were incubated with 20 ng/mL HRG with or without 1 μg/mL DHMEQ, 100 nM lapatinib, 100 nM gefitinib, 100 nM dasatinib or 100 nM sunitinib. The number of formed mammospheres was counted, and the percentage of mammosphere-forming cells was determined [data are mean ± SD; $n = 3$, $^{**}P < 0.01$, relative to the values in the HRG(+)]. (*C*) To examine the combinatory effect of DHMEQ and lapatinib, MCF7 cells were incubated with 20 ng/mL HRG with or without the indicated concentration of DHMEQ and lapatinib (data are mean ± SD; $n = 3$, $^{*}P < 0.05$, $^{**}P < 0.01$).

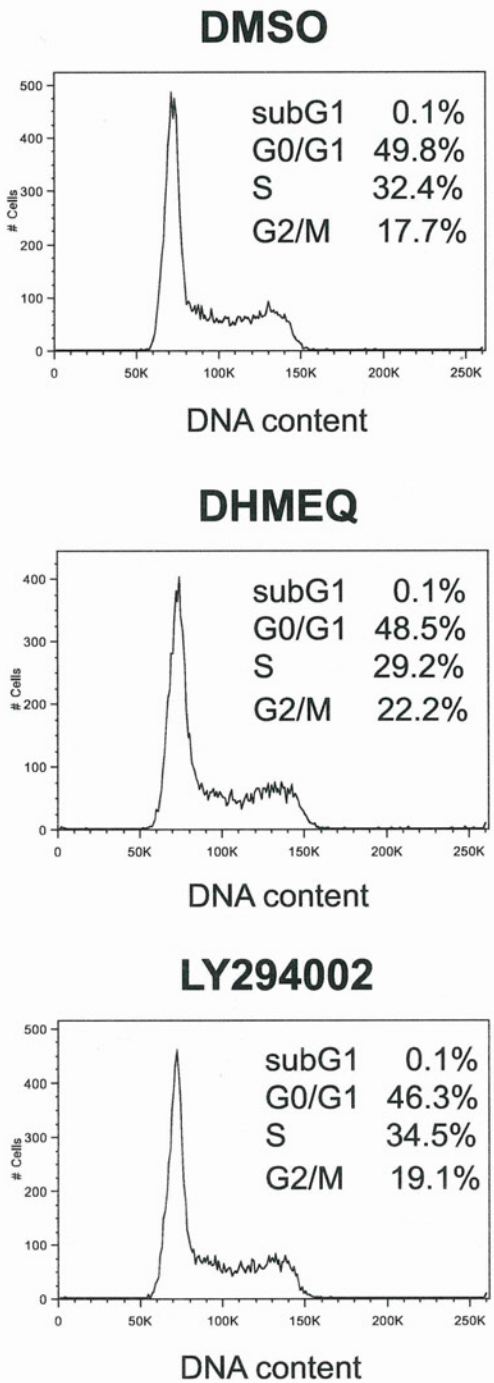

Fig. S3. Determination of apoptosis by DHMEQ in MCF7 mammosphere cells. To elucidate the apoptotic effect of DHMEQ, HRG-induced MCF7 mammosphere cells were incubated with DMSO, 1 μg/mL of DHMEQ, or 1 μM LY294002 for 4 d. Ethanol-fixed cells were then stained with propidium iodide (PI) and subjected to DNA content analysis by flow cytometry. The percentages of cells in the sub G1, G0/G1, S, and G2/M phase are indicated. DHMEQ and LY294002 had no effect on apoptosis (sub G1) at the effective concentrations for mammosphere formation.

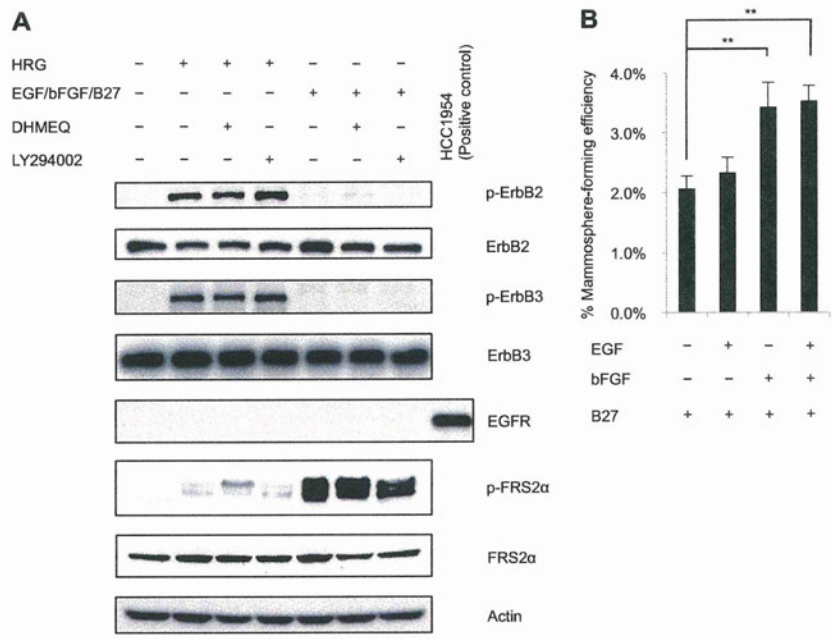

Fig. S4. The role of FGF signaling on mammosphere formation. (*A*) MCF7 mammosphere cells were treated with 5 μg/mL DHMEQ or 5 μM LY294002 for 1 h, and then the cells were treated with 20 ng/mL HRG or EGF/bFGF/B27 for 30 min. Protein expression levels were determined by immunoblotting. HRG induced the phosphorylation of ErbB2 and ErbB3, whereas EGF/bFGF/B27 did not. Treatment with EGF/bFGF/B27 induced the phosphorylation of FRS2α, a membrane-anchored docking protein involved in the activation of FGF receptor signaling. (*B*) MCF7 cells were incubated with B27 in combination with EGF, bFGF, or both, and the formed mammospheres were counted. Treatment with bFGF increased mammosphere formation (data are mean ± SD; $n = 3$, $^{**}P < 0.01$).

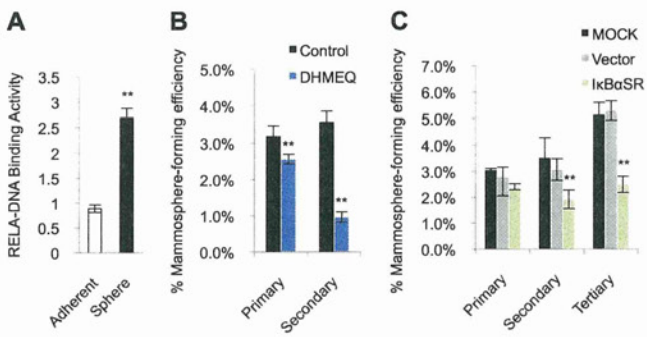

Fig. S5. The role of NF-κB on mammosphere formation in EGF/bFGF/B27-containing medium. (*A*) The DNA-binding activity of RELA was quantified by ELISA (data are mean ± SD; $n = 3$, $^{**}P < 0.01$) in the parental cells growing in 2D adherent culture and sphere cells cultured with EGF/bFGF/B27. (*B*) MCF7 cells were incubated with EGF/bFGF/B27 with or without 5 μg/mL DHMEQ. The formed primary mammospheres were dissociated into single cells and grown as secondary mammospheres without treatment with DHMEQ. The formed mammospheres were counted, and the percentage of mammosphere-forming cells was determined (data are mean ± SD; $n = 4$, $^{**}P < 0.01$, relative to the values in the respective controls). (*C*) MCF7 cells expressing the indicated lentiviral vectors were incubated with EGF/bFGF/B27, and the formed primary mammospheres were dissociated into single cells and grown as secondary mammospheres. This process was repeated three times. The percentage of mammosphere-forming cells was determined (data are mean ± SD; $n = 4$, $^{**}P < 0.01$, relative to the values in the respective controls).

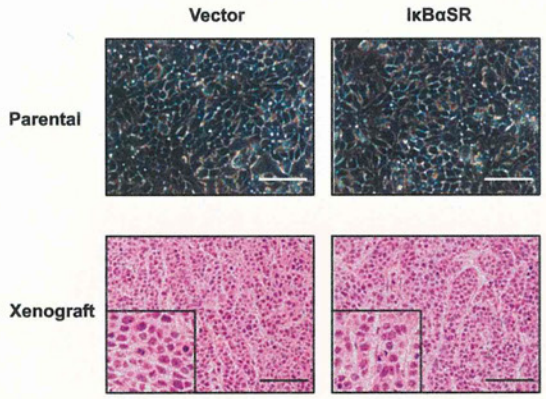

Fig. S6. Morphology of MCF7 cells expressing mutant IκBα or control vector in in vitro and histological findings of xenografted tumors. (*Upper*) Phase-contrast images of MCF7 cells expressing the control vector (*Left*) and mutant IκBα (*Right*). (*Lower*) Hematoxylin/eosin (H&E)–stained sections of tumor xenografts derived from MCF7 cells. NOD/SCID mice injected with these cells were killed after 3 wk. Scale bar = 100 μm. Both tumors showed similar histological findings. The tumors displayed a trabecular structure, and tumor cells possessed large round nuclei. In addition, both tumors had a similar mitotic index (average 4/HPF).

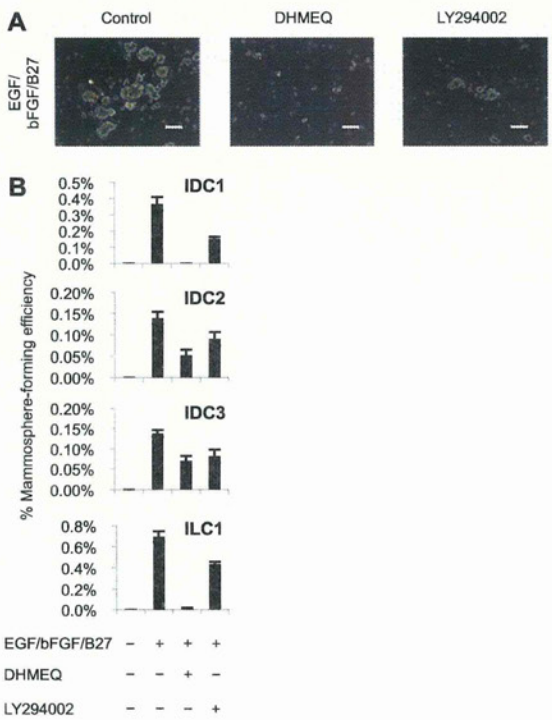

Fig. S7. NF-κB and PI3K signals control mammosphere formation of primary tumor cells derived from breast cancer patients in EGF/bFGF/B27-containing medium. (*A*) Representative images of primary cultures of mammospheres incubated with EGF/bFGF/B27, together with 5 μg/mL DHMEQ and 5 μM LY294002. Scale bar = 100 μm. (*B*) Cells from three invasive ductal carcinoma (IDC) patients (IDC1, 2, and 3) and one invasive lobular carcinoma (ILC) patient (ILC1) were treated as indicated in *A*, and the percentage of mammosphere-forming cells was determined (data are mean ± SD; $n = 4$).

Table S1. Characteristics of the patients

Patient	Age (y)	Diagnosis	Stage	Tumor size (cm)	ErbB2
IDC1	72	Invasive ductal carcinoma	IIA	2.5 × 2.0 × 2.0	1+
IDC2	87	Invasive ductal carcinoma	IIA	3.5 × 3.0 × 2.5	0–1+
IDC3	58	Invasive ductal carcinoma	IIA	2.5 × 2.0 × 1.5	1+
ILC1	72	Invasive lobular carcinoma	IA	1.6 × 1.5 × 1.5	1+

ErbB2, ErbB2 expression level (0–3+).

Int J Hematol (2012) 95:409–419
DOI 10.1007/s12185-012-1026-9

ORIGINAL ARTICLE

Efficacy and safety of nilotinib in Japanese patients with imatinib-resistant or -intolerant Ph+ CML or relapsed/refractory Ph+ ALL: a 36-month analysis of a phase I and II study

Kensuke Usuki · Arinobu Tojo · Yasuhiro Maeda · Yukio Kobayashi · Akira Matsuda · Kazuma Ohyashiki · Chiaki Nakaseko · Tatsuya Kawaguchi · Hideo Tanaka · Koichi Miyamura · Yasushi Miyazaki · Shinichiro Okamoto · Kenji Oritani · Masaya Okada · Noriko Usui · Tadashi Nagai · Taro Amagasaki · Aira Wanajo · Tomoki Naoe

Received: 22 August 2011 / Revised: 31 January 2012 / Accepted: 31 January 2012 / Published online: 23 February 2012

Abstract Although the tyrosine kinase inhibitor (TKI) imatinib is often used as first-line therapy for newly diagnosed chronic myelogenous leukemia (CML), some patients fail to respond, or become intolerant to imatinib. Nilotinib is a potent and selective second-generation TKI, with confirmed efficacy and tolerability in patients with imatinib-resistant or -intolerant CML. A phase I/II study was conducted in Japanese patients with imatinib-resistant or -intolerant CML or relapsed/refractory Ph+ acute lymphoblastic leukemia. Thirty-four patients were treated with nilotinib for up to 36 months. Major cytogenetic response was achieved in 15/16 patients (93.8%) with chronic-phase CML within a median of approximately 3 months. Major molecular response was achieved in 13/16 patients (81.3%). These responses were sustained at the time of the most recent evaluation in 13 patients and 11 patients, respectively. Hematologic and cytogenetic responses were also observed in patients with advanced CML. The BCR-ABL mutation associated with the most resistance to available TKIs, T315I, was observed in three patients. Common adverse events included rash, nasopharyngitis, leukopenia, neutropenia, thrombocytopenia, nausea, headache and vomiting. Most adverse events resolved following nilotinib dose interruptions/reductions. These results support the favorable long-term efficacy and tolerability of nilotinib in Japanese patients with imatinib-resistant or -intolerant chronic-phase chronic myeloid leukemia.

Electronic supplementary material The online version of this article (doi:10.1007/s12185-012-1026-9) contains supplementary material, which is available to authorized users.

This trial is registered at http://www.clinicaltrials.gov, number NCT01279473.

K. Usuki (✉)
Division of Hematology, NTT Kanto Medical Center,
5-9-22 Higashigotanda, Shinagawa-ku, Tokyo, Japan
e-mail: usuki@east.ntt.co.jp

A. Tojo
The Institute of Medical Science,
The University of Tokyo, Tokyo, Japan

Y. Maeda
Kinki University School of Medicine, Osaka, Japan

Present Address:
Y. Maeda
National Hospital Organization Osaka
Minami Medical Center, Osaka, Japan

Y. Kobayashi
National Cancer Center Hospital, Tokyo, Japan

A. Matsuda
International Medical Center, Saitama Medical University,
Saitama, Japan

K. Ohyashiki
Tokyo Medical University Hospital, Tokyo, Japan

C. Nakaseko
Chiba University Hospital, Chiba, Japan

T. Kawaguchi
Kumamoto University Hospital, Kumamoto, Japan

H. Tanaka
Hiroshima University Hospital, Hiroshima, Japan

Present Address:
H. Tanaka
Hiroshima City Asa Hospital, Hiroshima, Japan

Keywords Chronic myeloid leukemia · Acute lymphoblastic leukemia · Tyrosine kinase inhibitors · Nilotinib

Introduction

The tyrosine kinase inhibitor (TKI) imatinib (ST1571, Glivec™; Novartis) has been shown to induce durable responses in a high proportion of patients with chronic-phase chronic myeloid leukemia (CML-CP) [1–5]. However, disease progression caused by resistance to imatinib occurs in some CML patients treated with this drug [6].

CML patients in the accelerated phase (CML-AP) or in blast crisis (CML-BC) also show a complete cytogenetic response (CCyR) following treatment with imatinib, but the proportion of such patients achieving CCyR is considerably lower than that of CML-CP patients [7, 8]. Moreover, imatinib resistance and relapse are also common in CML-AP and -BC patients [6, 9]. Imatinib is also used to treat patients with Philadelphia chromosome-positive (Ph+) acute lymphoblastic leukemia (ALL), and many of these patients also achieve CCyR. However, the CCyRs in these patients are not sustained for as long as they are in CML-CP patients, both in Japan [10] and in other countries [11].

Approximately half of the cases of imatinib resistance are now known to result from mutations in *BCR-ABL* [12–16], which make particular leukemic cells resistant to BCR-ABL tyrosine kinase inhibition by imatinib.

K. Miyamura
Japanese Red Cross Nagoya First Hospital, Nagoya, Japan

Y. Miyazaki
Nagasaki University Hospital, Nagasaki, Japan

S. Okamoto
Keio University Hospital, Tokyo, Japan

K. Oritani
Osaka University Hospital, Osaka, Japan

M. Okada
Hyogo College of Medicine, Hyogo, Japan

N. Usui
The Jikei University Daisan Hospital, Tokyo, Japan

T. Nagai
Jichi Medical University Hospital, Tochigi, Japan

T. Amagasaki · A. Wanajo
Novartis Pharma Japan, Tokyo, Japan

T. Naoe
Nagoya University Hospital, Nagoya, Japan

Nilotinib (AMN107, Tasigna®; Novartis) is a second-generation TKI that inhibits BCR-ABL-dependent cell proliferation and induces cell death in BCR-ABL phenotypic cells [17, 18]. Nilotinib was originally approved as second-line treatment for imatinib-resistant or -intolerant CML-CP and -AP patients [19–22]. More recently, it was approved as first-line therapy for CML-CP and -AP patients [23, 24] in Japan. Several studies have reported hematologic response (HR) and cytogenetic response (CyR) with nilotinib in patients with imatinib-resistant or -intolerant CML-BC and those with relapsed/refractory Ph+ ALL [25, 26].

We recently reported the results of a phase I and II study of nilotinib in which Japanese patients with imatinib-resistant or -intolerant Ph+ CML, or relapsed/refractory Ph+ ALL were treated for up to 12 months [22]. Here, we report the effects of treatment with nilotinib for up to 36 months in these patients, as well as the results of mutation analysis and the response by BCR-ABL mutation status.

Materials and methods

Study design and objectives

This was an open-label, multicenter, continuous-dose, 36-month extension of a phase I and II clinical study. The study protocol and documentation were approved by the institutional review boards of each participating center. The observation period was defined to be 36 months, including the entire 3 months of the Ph I/II clinical study. The study was conducted in accordance with the ethical principles established by the Declaration of Helsinki and in compliance with institutional guidelines.

The primary objective of this extension study was to evaluate the long-term safety of nilotinib, including chronic toxicity. Secondary objectives included the long-term efficacy of nilotinib, the relationship between BCR-ABL mutations or BCR-ABL transcript levels determined by quantitative RT-PCR, and the clinical efficacy of nilotinib. The time of last evaluation in this study was the time at which patients had received treatment for more than 3 years or the time at which the drug became commercially available at each of the study institutions, whichever was the later.

Patients

The inclusion and exclusion criteria are described in the original study report [22]. Briefly, Japanese patients were eligible if they had imatinib-resistant or -intolerant CML-CP, CML-AP, CML-BC or relapsed/refractory Ph+ ALL, were at least 20 years of age, had a World Health Organization (WHO) performance status (PS) ≤2, and had normal hepatic, renal and cardiac function.

Treatments

Nilotinib 400 mg was administered orally twice daily. Patients were required to fast for 2 h before and after each dose. One treatment course (1 cycle) was defined as 28 consecutive days of twice-daily nilotinib. If administration was delayed for more than 21 days (42 days for hematologic toxicity) after the previous dose, the patient was withdrawn from the study. Dose reductions to 400 mg once daily (one level lower than the standard dose) or 200 mg once daily (two levels lower than the standard dose) were permitted. The nilotinib dose at re-introduction was one level lower than that at cessation. The mean dose in each patient was calculated by assuming the dose during the cessation period to be 0 mg.

Treatment with nilotinib was continued until disease progression or unacceptable toxicity was observed, or at the investigator's discretion that treatment be discontinued. After the regulatory approval date for nilotinib in Japan (January 29, 2009), its administration was continued for longer than 3 years or until the drug became commercially available, whichever was later.

Measurements

Response rates

Criteria for HR and CyR were similar to those reported elsewhere [19, 21, 27] and are described in more detail in Tojo et al. [22]. Briefly, CyR was determined as the percentage of Ph+ cells of ≥20 cells in the metaphase in each bone marrow sample, and was classified as complete (0% Ph+ cells), partial (1–35% Ph+ cells), minor (36–65% Ph + cells) or minimal (66–95% Ph+ cells). Major CyR (MCyR) included complete and partial CyR. Fluorescent in situ hybridization was used if <20 cells were examined or if the bone marrow sample was not adequate for assessment.

The proportion of patients who experienced major molecular response (MMR) was also determined for each disease phase and subtype. BCR-ABL transcript levels were measured by quantitative RT-PCR and reported in the international scale using a conversion factor of 1.25 established by the Institute of Medical and Veterinary Science, Australia. MMR was defined as a BCR-ABL/BCR ratio ≤0.1%. Loss of MMR was defined as a BCR-ABL/BCR ratio >0.1%. Patients with MMR at baseline were considered "not evaluable" and were excluded from the analysis. Only evaluable patients in the intention-to-treat (ITT) population were included in the analyses of overall response rates.

Patients whose BCR-ABL transcript levels were not evaluated at baseline were considered "not assessable", and were not included in the denominator when calculating the proportion of patients who achieved MMR.

Mutation analysis

Efficacy was also examined based on the subtype of BCR-ABL mutation at baseline and after nilotinib administration. Mutation analysis was performed by the direct sequence identification method. The number and proportion of patients with HR, CyR or MMR were calculated for the following categories of mutation [22]: no mutation, any mutation, multiple mutations, P-loop mutations (amino acids 248–255), non-P-loop mutations, and protocol-specified subgroup mutations associated with imatinib resistance mutations (L248, Q252, T315, F317, H396, M237, M244, G250, D325, S348, M351, E355, A380, L387, M388, F486, Y253, E255, and F359). The impact of baseline mutations or development of new mutations on patient outcomes was assessed.

Safety analyses

Safety assessment included an evaluation of the frequency and severity of adverse events, which included hematologic and biochemical laboratory tests, vital signs, physical examinations (including body weight), WHO PS, cardiac function tests (12-lead ECG, cardiac enzyme test, echocardiography), and chest X-rays, as needed. Adverse events were graded according to the National Cancer Institute Common Terminology Criteria for Adverse Events (version 3.0). The monitoring was continued for at least 28 days after the last dose of nilotinib.

Statistical analyses

The ITT population was used for the efficacy analysis and was pre-specified as all patients enrolled in either the phase I or phase II studies, and who were treated with nilotinib 400 mg twice daily, irrespective of when they withdrew from the study. The safety (SAF) population comprised all patients in the ITT population who underwent safety assessments. HR, CyR and MMR were summarized by disease phase and subtype (CML-CP, CML-AP, CML-BC, and Ph+ ALL). The time to first response and duration of response were assessed by descriptive statistics or Kaplan–Meier analysis, as appropriate. No statistical comparisons were made.

Results

Patients and treatment administration

This 36-month study included 34 Japanese patients with imatinib-resistant or -intolerant CML (CML-CP, $N = 16$; CML-AP, $N = 7$; CML-BC, $N = 4$) or Ph+ ALL ($N = 7$).

Thirty-one patients were enrolled into the phase II study and treated with nilotinib 400 mg twice daily (CML-CP: 14, CML-AP: 7, CML-BC: 3; Ph+ ALL: 7) and 3 patients were enrolled in the phase I study and treated with nilotinib 400 mg twice daily (CML-CP: 2; CML-BC: 1) [22]. The characteristics and disposition of patients are summarized in Tables 1 and 2, respectively. Fourteen patients (CML-CP: 13; CML-AP: 1) received nilotinib until the end of the study while 20 patients (CML-CP: 3, CML-AP: 6, CML-BC: 4; Ph+ ALL: 7) discontinued study treatment. The

Table 1 Patient characteristics (ITT population)

	CML-CP ($N = 16$)	CML-AP ($N = 7$)	CML-BC ($N = 4$)	Ph+ ALL ($N = 7$)	Total ($N = 34$)
Age (years)	57.0 (30–83)	61.0 (30–74)	53.0 (29–70)	62.0 (23–80)	61.5 (23–83)
Sex					
Male	9 (56)	5 (71)	2 (50)	6 (86)	22 (65)
Female	7 (44)	2 (29)	2 (50)	1 (14)	12 (35)
Body weight (kg)	61.2 (44.5–89.0)	64.8 (49.1–83.0)	63.3 (35.5–69.0)	55.8 (46.2–60.2)	60.5 (35.5–89.0)
WHO PS					
0	16 (100)	4 (57)	2 (50)	4 (57)	26 (76)
1	0 (0)	2 (29)	2 (50)	3 (43)	7 (21)
2	0 (0)	1 (14)	0 (0)	0 (0)	1 (3)
Time since first diagnosis (months)	30.4 (1.4–122.8)	108.6 (12.5–192.8)	65.3 (20.5–102.8)	16.2 (3.7–134.1)	30.4 (1.4–192.8)
Imatinib resistance	4 (25.0)	4 (57.1)	4 (100.0)	7 (100.0)	19 (55.9)
Imatinib intolerance	12 (75.0)	3 (42.9)	0 (0.0)	0 (0.0)	15 (44.1)
Highest imatinib dose (mg)	500 (200–800)	800 (400–800)	700 (600–800)	600 (600–600)	600 (200–800)

Values are *n* (%) or median (range)

ITT intention-to-treat, *WHO PS* World Health Organization performance status

Table 2 Patient disposition (ITT population)

	CML-CP ($N = 16$)	CML-AP ($N = 7$)	CML-BC ($N = 4$)	Ph+ ALL ($N = 7$)	Total ($N = 34$)
Completed the long-term study	13 (81)	1 (14)	0 (0)	0 (0)	14 (41)
Discontinued treatment and withdrawn from the study	3 (19)	6 (86)	4 (100)	7 (100)	20 (59)
Reason for discontinuation					
Adverse event(s)	0 (0)	1 (14)	1 (25)	1 (14)	3 (9)
Allo-HSCT performed	1 (6)	2 (29)	1 (25)	0 (0)	4 (12)
Disease progression	1 (6)	3 (43)	2 (50)	6 (86)	12 (35)
Withdrawal of consent	1 (6)	0 (0)	0 (0)	0 (0)	1 (3)
Dose reduction	15 (94)	5 (71)	3 (75)	4 (57)	27 (79)
Withdrawal from treatment	11 (69)	2 (29)	2 (50)	2 (29)	17 (50)
Drug administration recommenced at a reduced dose after withdrawal	10 (63)	1 (14)	0 (0)	2 (29)	13 (38)
Duration of exposure (days)[a]	1099.5 (176–1173)	84.0 (56–1099)	133.0 (15–247)	56.0 (13–644)	445.5 (13–1173)
Duration of administration (days)[b]	1084.5 (165–1173)	84.0 (28–1099)	126.5 (14–247)	56.0 (13–609)	428.0 (13–1173)
Daily dose (mg)[c]	612.9 (394.2–798.6)	789.6 (284.9–797.5)	742.6 (402.4–798.4)	785.7 (483.2–794.1)	750.7 (284.9–798.6)

Values are *n* (%) or median (range)

Allo-HSCT allogeneic hematopoietic stem cell transplantation, *ITT* intention-to-treat

[a] Includes drug interruptions

[b] Excludes drug interruptions

[c] Daily dose = total dose/duration of exposure (includes drug interruption)